Journal of the American Heart Association

ORIGINAL RESEARCH

Tetrodotoxin-Sensitive Neuronal-Type Na^+ Channels: A Novel and Druggable Target for Prevention of Atrial Fibrillation

Mark A. Munger, PharmD; Yusuf Olğar, PhD; Megan L. Koleske, BS; Heather L. Struckman, BS; Jessica Mandrioli, MD; Qing Lou, PhD; Ingrid Bonila, PhD; Kibum Kim, PhD; Roberto Ramos Mondragon, PhD; Silvia G. Priori, MD, PhD; Pompeo Volpe, MD; Héctor H. Valdivia, MD, PhD; Joseph Biskupiak, PhD; Cynthia A. Carnes, PharmD, PhD; Rengasayee Veeraraghavan, PhD; Sándor Györke, PhD; Przemysław B. Radwański, PharmD, PhD

BACKGROUND: Atrial fibrillation (AF) is a comorbidity associated with heart failure and catecholaminergic polymorphic ventricular tachycardia. Despite the Ca^{2+}-dependent nature of both of these pathologies, AF often responds to Na^+ channel blockers. We investigated how targeting interdependent Na^+/Ca^{2+} dysregulation might prevent focal activity and control AF.

METHODS AND RESULTS: We studied AF in 2 models of Ca^{2+}-dependent disorders, a murine model of catecholaminergic polymorphic ventricular tachycardia and a canine model of chronic tachypacing-induced heart failure. Imaging studies revealed close association of neuronal-type Na^+ channels (nNa_v) with ryanodine receptors and Na^+/Ca^{2+} exchanger. Catecholamine stimulation induced cellular and in vivo atrial arrhythmias in wild-type mice only during pharmacological augmentation of nNa_v activity. In contrast, catecholamine stimulation alone was sufficient to elicit atrial arrhythmias in catecholaminergic polymorphic ventricular tachycardia mice and failing canine atria. Importantly, these were abolished by acute nNa_v inhibition (tetrodotoxin or riluzole) implicating Na^+/Ca^{2+} dysregulation in AF. These findings were then tested in 2 nonrandomized retrospective cohorts: an amyotrophic lateral sclerosis clinic and an academic medical center. Riluzole-treated patients adjusted for baseline characteristics evidenced significantly lower incidence of arrhythmias including new-onset AF, supporting the preclinical results.

CONCLUSIONS: These data suggest that nNa_vs mediate Na^+-Ca^{2+} crosstalk within nanodomains containing Ca^{2+} release machinery and, thereby, contribute to AF triggers. Disruption of this mechanism by nNa_v inhibition can effectively prevent AF arising from diverse causes.

Key Words: atrial arrhythmias ■ atrial fibrillation ■ cardiac arrhythmias ■ neuronal-type Na^+ channel blockade

Atrial arrhythmia, such as atrial fibrillation (AF), is a leading cause of morbidity and mortality in the United States.[1] It is a common comorbidity associated with heart failure and its risk has been associated with "leaky" ryanodine receptor 2 (RyR2) Ca^{2+} release channels.[2–4] The importance of leaky RyR2 to atrial arrhythmogenesis is particularly evident in patients with catecholaminergic polymorphic ventricular tachycardia (CPVT).[5] In this pathology, mutations in RyR2 or in the sarcoplasmic reticulum (SR) Ca^{2+}-binding protein calsequestrin increase propensity for AF.[6] Emerging evidence also suggests that the link between Ca^{2+} handling and atrial arrhythmias is in part modulated by Na^+ influx.[7]

The predominant Na^+ channel (Na_v) isoform found in the heart ($Na_v1.5$) is decreased in cardiomyopathy, as well as in AF.[7,8] However, tetrodotoxin-sensitive neuronal-type Na^+ channels (nNa_vs) are upregulated

Correspondence: Przemysław B. Radwański, PharmD, PhD, Davis Heart and Lung Research Institute, The Ohio State University, 460 Medical Center Drive, IBMR 415C, Columbus, OH 43210. E-mail: radwanski.2@osumc.edu

Supplementary Materials for this article are available at https://www.ahajournals.org/doi/suppl/10.1161/JAHA.119.015119

For Sources of Funding and Disclosures, see page 12.

JAHA is available at: www.ahajournals.org/journal/jaha

CLINICAL PERSPECTIVE

What Is New?

- Riluzole, a neuronal type Na^+ channel blocker, was investigated in 2 retrospective amyotrophic lateral sclerosis cohorts.
- Patients treated with riluzole had significantly lowered incidence of arrhythmias, including new-onset atrial fibrillation.

What Are the Clinical Implications?

- The pharmacological class of neuronal-type Na^+ channel blockade may offer a unique mechanism to prevent arrhythmias including atrial fibrillation.

Nonstandard Abbreviations and Acronyms

AF	atrial fibrillation
ALS	amyotrophic lateral sclerosis
CPVT	catecholaminergic polymorphic ventricular tachycardia
I_{Na}	Na^+ current
ISO	isoproterenol
Na_v	Na^+ channel
nNa_v	neuronal Na^+ channel
NCX	Na^+/Ca^{2+} exchange
RyR2	ryanodine receptor
SR	sarcoplasmic reticulum
WT	wild-type

in these pathologies resulting in enhanced persistent Na^+ current (I_{Na}).[7,9] The subcellular localization of different Na_V isoforms thus determines the location of late Na^+ entry relative to Ca^{2+}-handling machinery. This, in turn, may determine whether nNa_v-mediated Na^+/Ca^{2+} exchange (NCX) merely contributes to global cytosolic Ca^{2+} overload or acts directly to trigger abnormal Ca^{2+} release.[10–12]

Ventricular proarrhythmia is an important limitation of current drug therapies used in AF.[13–15] Thus, the identification of agents that safely and effectively prevent arrhythmogenic trigger in the atria is imperative. Riluzole, an nNa_v inhibitor used to manage amyotrophic lateral sclerosis (ALS),[16] effectively suppresses triggered ventricular arrhythmias in multiple animal models.[10,17–19] Given its extensive safety profile,[20] riluzole could potentially safely prevent AF. Here, we provide evidence from preclinical models and patients suggesting riluzole as a safe and effective treatment for atrial arrhythmias.

METHODS

Expanded methods are available in Data S1.

The preclinical and retrospective cohort data that support the findings of this study are available from the corresponding author and Dr Mark Munger (mark.munger@hsc.utah.edu), respectively, upon reasonable request.

Study Approval

All animal procedures were approved by The Ohio State University and University of Michigan Institutional Animal Care and Use Committees and conformed to the *Guide for the Care and Use of Laboratory Animals* published by the US National Institutes of Health (publication No. 85-23, revised 2011). The historical cohort was reviewed and approved as exempt following applicable guidelines involving the ethical treatment of human subjects by the University of Utah's institutional review board before the initiation of data collection. The University of Utah's institutional review board is fully accredited by the Human Research Protection Program.

Preclinical Evaluation of Antiarrhythmic Targeting of nNa_vs

Atrial cardiomyocytes, obtained from cardiac calsequestrin mutant (R33Q) wild-type (WT) mice or failing canine hearts were enzymatically dissociated for patch-clamp recordings, confocal immunolabeling, or Ca^{2+} imaging. A subset of mice was used to assess the role of nNa_vs in an in vivo arrhythmia induction.

Clinical Evaluation of Antiarrhythmic Targeting of nNa_vs

We conducted a retrospective cohort study of patients with ALS who were treated with riluzole (study group) versus no riluzole (control group) from the ALS Centre of the Azienda Ospedaliero, Universitaria di Modena, Modena, Italy, and the University of Utah, Salt Lake City, Utah. Data were collected through queries of structured data fields. Variables extracted from structured fields included demographic information (ie, age on the index date, sex, race, and body mass index), laboratory results, diagnostic tests and results, prescription records, and hospitalizations with cardiovascular encounter(s) including acute coronary syndrome, acute myocardial infarction, heart failure, and any arrhythmia including atrial flutter or fibrillation. Race and ethnicity were grouped into white, black, Hispanic, Asian, and other/unknown. Cardiovascular risk factors and specific medications for cardiovascular risk prevention and treatment were collected and identified. Distribution of the clinical and demographic characteristics of the study cohort

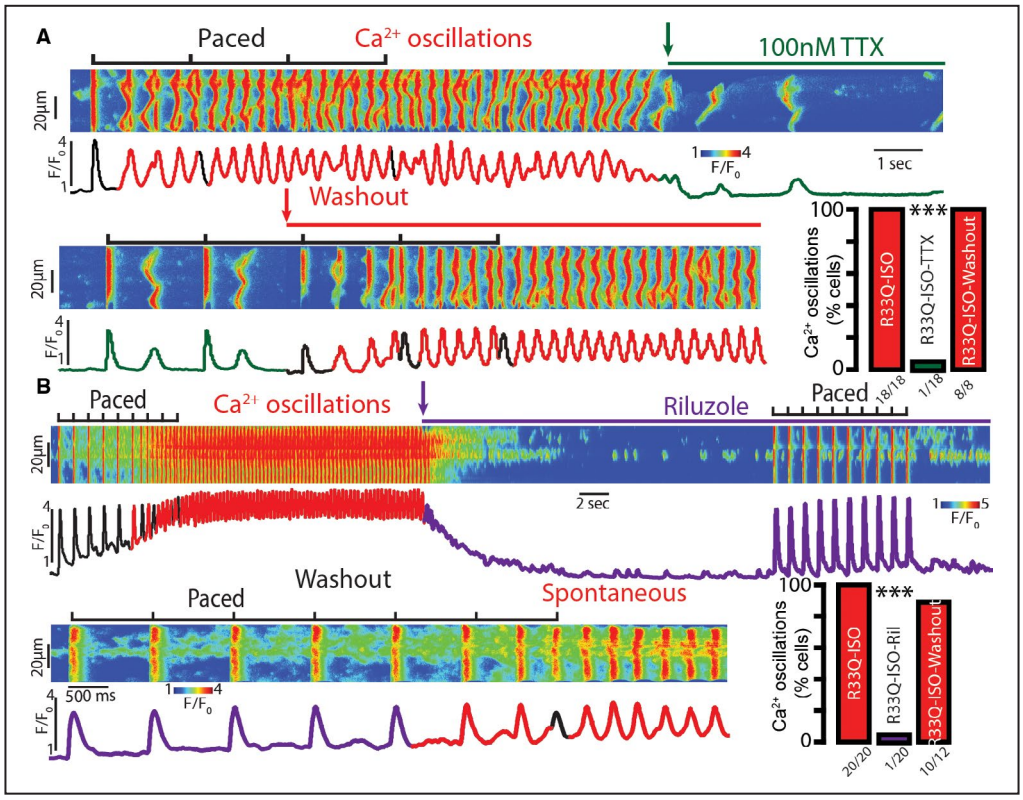

Figure 1. Inhibition of tetrodotoxin (TTX)-sensitive neuronal Na_Vs (nNa_Vs) is sufficient to prevent induction of aberrant, repetitive Ca^{2+} oscillations in R33Q atrial myocytes.
A, Representative examples of the line scan images and corresponding Ca^{2+} transients recorded in field-stimulated R33Q atrial cardiomyocytes paced at 0.5 Hz and loaded with the Ca^{2+} indicator, Fluo-3 AM. Cells were treated with isoproterenol (ISO, 100 nmol/L) and subsequently TTX (100 nmol/L; green arrow indicates time when TTX was added) was rapidly applied. β-Adrenergic stimulation with ISO promoted aberrant, repetitive Ca^{2+} oscillations (median pacing frequency was 2 Hz with the range of 0.5 to 4 Hz), while TTX (100 nmol/L) significantly decreased their incidence. Ca^{2+} oscillations were induced after drug washout (red arrow; number of cells tested depicted under the corresponding bars, N=8 animals for ISO and ISO-TTX, N=6 animals for ISO-washout, respectively; ***P<0.0001 McNemar test for ISO vs ISO-TTX, P<0.0001 Fisher exact test for ISO-TTX vs ISO-washout). **B**, Treatment of ISO (100 nmol/L)-exposed R33Q atrial myocytes with 10 µmol/L riluzole (Ril) significantly reduced the incidence of aberrant, repetitive Ca^{2+} oscillations, an effect that was washable (median pacing frequency was 2 Hz with the range of 0.5 to 7 Hz; number of cells tested depicted under the corresponding bars, N=10 animals for ISO and ISO-Ril, N=8 animals for ISO-washout, respectively; ***P<0.0001 McNemar test for ISO vs ISO-Ril, P<0.0001 Fisher exact test for ISO-Ril vs ISO-washout).

were described among the overall cohort from both the Italian and US databases, and among riluzole versus no-riluzole users. Baseline characteristics between the riluzole and no-riluzole groups were compared using chi-square test, and Fisher exact test if the number of patients having a specific clinical character was <5. Cardiac pacemaker and implantable cardioverter-defibrillator placement were collected, if applicable, and cardiac monitoring for AF was conducted based on patient presentation of symptoms.

The primary clinical end point was a composite of arrhythmia and AF. The time-to-end point from the first exposure to riluzole or earliest available date on or after the diagnosis of ALS, if no riluzole cohort, was projected using Kaplan–Meier curves where patients were censored when they encountered the end point or at the last follow-up from each institution. The measure of treatment effect was hazard ratio (HR) and 95% CI estimate from Cox proportional hazard regression model under intention-to-treat principles (ie, post-index date variables were not incorporated into the analysis such as medication adherence) where the effect measure was adjusted for the baseline characteristics that were marginally different (P<0.1) between the riluzole and no-riluzole groups. The analysis was performed for the overall cohort, then limited to the Utah cohort to qualitatively examine the influence of the heterogeneity across the Italy and US cohorts on the measure of treatment effect. All tests were 2-tailed with an α of 0.05 for statistical significance. Data analysis was conducted with SAS version 9.4 (SAS Institute Inc).

RESULTS

nNa_v Blockade Prevents Leaky RyR2-Induced Aberrant Ca^{2+} Oscillations

We first determined whether nNa_v exerts a unique action on intracellular Ca^{2+} handling, which may contribute to atrial arrhythmia initiation. Exposure of calsequestrin-associated CPVT atrial myocytes to isoproterenol (100 nmol/L) induced self-sustaining, repetitive Ca^{2+} oscillations, consistent with previous findings.[6] These oscillations were abolished by tetrodotoxin (100 nmol/L; Figure 1A). Further, tetrodotoxin prevented induction of repetitive Ca^{2+} oscillations by field stimulation in the presence of isoproterenol in nearly all cells tested (Figure 1A), despite increasing SR Ca^{2+} load (Figure S1). However, field stimulation elicited Ca^{2+} oscillations in all cells upon washout of tetrodotoxin (Figure 1A).

Next, we compared tetrodotoxin with riluzole, an agent currently employed in the management of ALS.[21] At the resting potential, riluzole has been shown to preferentially block tetrodotoxin-sensitive nNa_vs in dorsal root ganglion neurons.[16] First, we examined the impact of riluzole on the tetrodotoxin-sensitive component of I_{Na}. Both 100 nmol/L tetrodotoxin and 10 μmol/L riluzole reduced peak I_{Na} density to similar degrees (peak I_{Na} at −35 mV of −36.4±3.7 pA/pF versus −25.8±4.4 and −28.1±3.0 pA/pF for control, riluzole and tetrodotoxin, respectively; P=0.0002 Kruskal–Wallis rank sum test; Figure S2A). Both also shifted steady-state inactivation of I_{Na} to more hyperpolarized potentials ($V_{1/2}$ of −87.2±3.7 mV versus −98.1±3.0 and −95.9±3.2 mV for R33Q, riluzole and tetrodotoxin, respectively; P=0.0345 Kruskal–Wallis rank sum test; Figure S2B). Importantly, riluzole, like tetrodotoxin, prevented aberrant Ca^{2+} oscillations (Figure 1B) and increased SR Ca^{2+} load (Figure S1). These data point to the antiarrhythmic efficacy in CPVT of nNa_v inhibition by riluzole, likely via suppression of late I_{Na} induced by isoproterenol. Under control conditions, we did not observe significant differences in late I_{Na} between WT and CPVT (Figures 2B and 5A). Upon addition of isoproterenol (100 nmol/L), CPVT atrial myocytes evidenced an increase in late I_{Na} (Figure 2B). Both peak as well as late I_{Na} were reduced by riluzole (Figure 2). Taken together, these data support a role for nNa_v in arrhythmogenic Ca^{2+} release in CPVT atria.

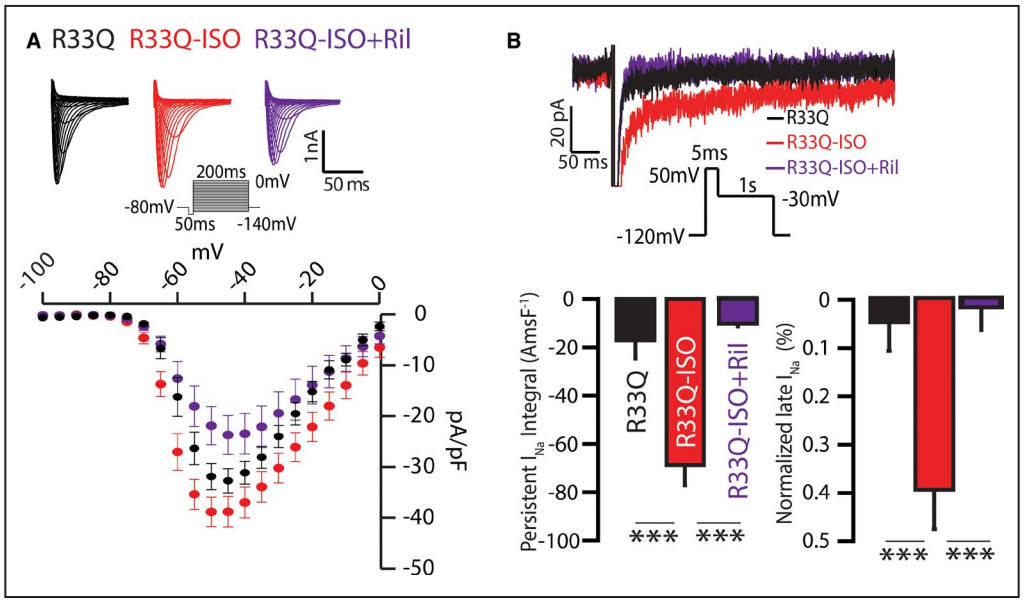

Figure 2. Effect of neuronal Na_v (nNa_v) blockade with riluzole (Ril) on isoproterenol (ISO)-promoted inward Na^+ currents (I_{Na}) in R33Q atrial myocytes.

A, Representative I_{Na} (top) were elicited by a protocol presented in the inset before (black) or after addition of ISO (100 nmol/L; red) or ISO (100 nmol/L)+Ril (10 μmol/L; purple). (Bottom) Corresponding current-voltage relationship from control, ISO, and ISO+Ril (n=10, 9, and 7 cells from 5, 6, and 5 mice, respectively). Addition of ISO+Ril reduced I_{Na} density relative to ISO alone (peak I_{Na} at −40 mV of −37.1±3.2 vs −22.4±3.9 pA/pF for ISO and ISO+Ril, respectively; P=0.0102 ANOVA, P=0.0418 for ISO vs ISO+Ril). **B**, Representative traces of persistent I_{Na} elicited using the protocol shown in the inset were recorded before (black) or after addition of ISO (100 nmol/L; red) or ISO+Ril (10 μmol/L; purple). ISO enhanced persistent I_{Na} in R33Q cardiomyocytes, while Ril suppressed β-adrenergic–mediated increase in persistent I_{Na} (n=9, 8, and 8 cells from 3, 3, and 4 mice for R33Q, ISO, and ISO-Ril, respectively; P<0.0001 ANOVA, ***P=0.0004 for persistent I_{Na} integral and ***P<0.0001 for normalized late I_{Na}). Summary data are presented as persistent I_{Na} integral Amp-ms/F (AmsF^{-1}; left) or normalized late I_{Na} (%; right), which were measured by either integrating I_{Na} between 50 and 450 ms (left) or normalizing mean persistent INa recorded between 250 and 450 ms by peak current generated by a step to −40 mV.

We also examined whether blockade of other Na_V isoforms and/or RyR2 in addition to tetrodotoxin-sensitive Na_V isoforms confers additional benefit beyond that achieved with 100 nmol/L tetrodotoxin. To that end, we used R-propafenone[22–25] (300 nmol/L) and ranolazine[26–29] (10 μmol/L) to assess their effect on cellular arrhythmia potential. At these concentrations, ranolazine and R-propafenone achieved similar levels of peak I_{Na} reduction relative to riluzole (peak I_{Na} at −40 mV of −22.4±3.9 pA/pF versus −23.9±2.7 pA/pF and −23.3±1.5 pA/pF for isoproterenol+riluzole versus isoproterenol+ranolazine and isoproterenol+R-propafenone, respectively; Figures 2A and 3A). Furthermore, both of these agents reduced induction of aberrant Ca^{2+} oscillations (Figure 3C and 3D). Notably, the extent of reduction in cellular arrhythmia propensity was proportional to the extent of late I_{Na} reduction achieved by these agents (Figure 3B), suggesting that nNav blockade is sufficient for the antiarrhythmic effect of Na_V blockers. Furthermore, the

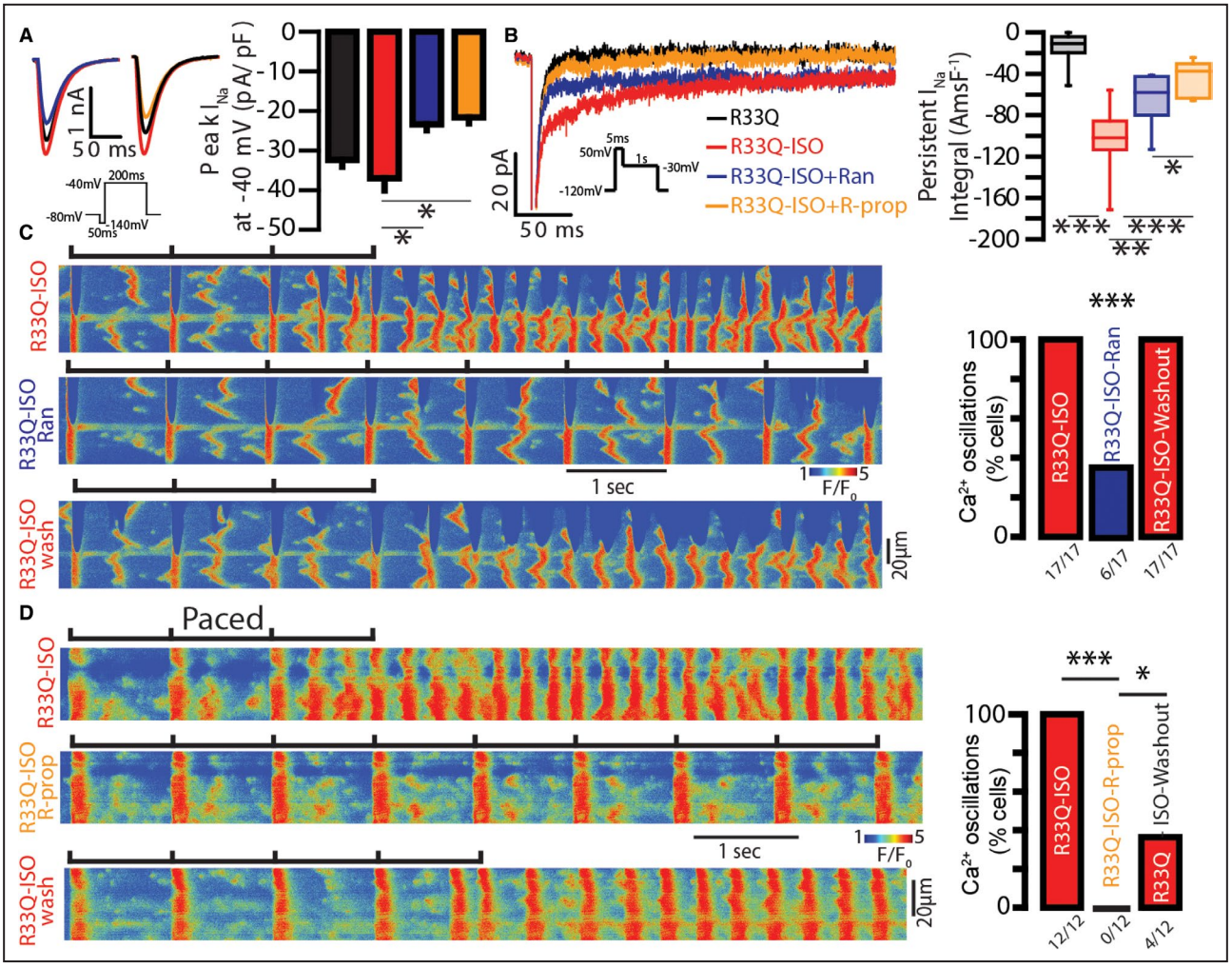

Figure 3. The extent of late inward Na^+ currents (I_{Na}) inhibition corresponds to prevention of aberrant, repetitive Ca^{2+} oscillations in R33Q atrial myocytes.

A, (Left) I_{Na} obtained by step protocol illustrated in 1-second intervals. (Right) In isoproterenol (ISO; 100 nmol/L)-treated R33Q atrial myocytes, addition of ranolazine (Ran; 10 μmol/L, blue trace and bar; n=5 from N=4 animals) or R-propafenone (R-prop; 300 nmol/L, orange trace and bar; n=4 from N=3 animals) significantly reduced peak I_{Na} (*P*=0.0016 ANOVA, **P*=0.0418 for ISO vs ISO+Ran and **P*=0.0246 for ISO vs ISO+R-prop) relative to ISO alone (n=7 from N=5 animals). Notably, there was no difference in peak I_{Na} reduction between the groups. **B**, (Left) Representative persistent I_{Na} elicited using the protocol shown in the inset. (Right) ISO (100 nmol/L) increased persistent I_{Na}, while Ran and R-prop reduced it (n=13, 13, 7, and 7 cells from 6, 6, 6 and 4 mice for R33Q, ISO, ISO+Ran, and ISO+R-prop, respectively; *P*<0.0001 ANOVA, ****P*<0.0001, ***P*=0.0082, and **P*=0.0480). Notably, R-prop reduced ISO-induced persistent I_{Na} to a greater extent than Ran (*P*=0.0480). **C**, Treatment of ISO (100 nmol/L)-exposed R33Q atrial myocytes with Ran (10 μmol/L) significantly reduced the incidence of aberrant, repetitive Ca^{2+} oscillations, which was washable (number of cells tested depicted under the corresponding bars, N=5 animals; ****P*=0.0009 McNemar test for ISO vs ISO-Ran and for ISO-Ran vs ISO-washout). **D**, R-prop abolished aberrant, repetitive Ca^{2+} oscillations, an effect that was only partially washable only after 10 minutes. (Number of cells tested depicted under the corresponding bars, N=4 animals; ****P*=0.0005 McNemar test for ISO vs ISO–R-prop, **P*=0.0455 for ISO–R-propafenone vs ISO-washout).

effects of these 2 compounds were, in part, washable (Figure 3C and 3D).

Next, we confirmed the importance of NCX to the proarrhythmic process in this model.[6,11] Acute NCX inhibition (5 mmol/L $NiCl_2$) abolished repetitive Ca^{2+} oscillations in all cells tested (Figure S3A). Since we were unable to electrically stimulate cardiomyocytes in the presence of $NiCl_2$, we repeated these experiments during NCX inhibition with SEA0400 (1 μmol/L). SEA0400 prevented induction of arrhythmogenic Ca^{2+} oscillations in over two thirds of cells tested (Figure S3B).

nNa$_v$s Closely Associate With Ca^{2+}-Handling Machinery

In order to examine close proximity of nNa$_v$ with SR Ca^{2+}-release machinery, which may contribute to aberrant Ca^{2+} release through NCX in atrial myocytes, we performed confocal microscopy. This approach identified multiple nNa$_v$ isoforms (Na$_v$1.1, Na$_v$1.3, and Na$_v$1.6) localized near RyR2 and NCX in atrial myocytes from R33Q hearts (Figure 4A and 4B, top). Proximity ligation assays[10] confirmed close association (within 40 nm)[30] of all 3 nNa$_v$ isoforms with RyR2 and NCX (Figure 4 and 4B, bottom). These results place nNa$_v$s near enough to leaky RyR2 to promote arrhythmias via aberrant NCX.

Augmentation of nNa$_v$ Activity is Proarrhythmic

Next, we examined whether augmented nNa$_v$–mediated Na^+ influx is sufficient to induce arrhythmogenic Ca^{2+} oscillations. Exposing WT myocytes to isoproterenol alone was insufficient to elicit Ca^{2+} oscillations. However, persistent I_{Na} induced by nNa$_v$ augmentation (β-pompilidotoxin, 40 μmol/L; Figure 5A)[10,31] promoted

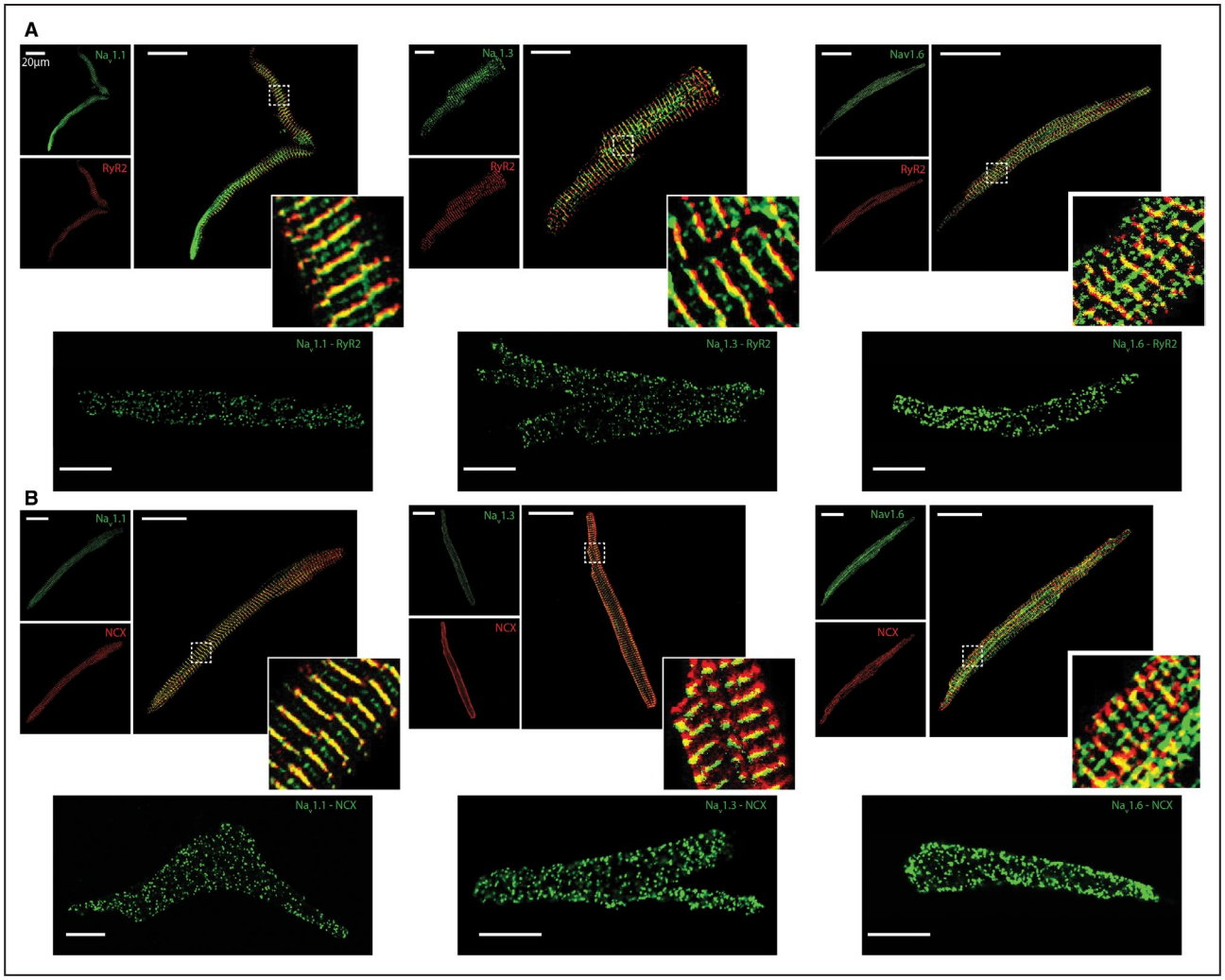

Figure 4. Neuronal Na^+ channel (nNa$_v$) and ryanodine receptor 2 (RyR2) colocalize to the same discrete subcellular regions. Representative confocal micrographs of myocytes isolated from R33Q mice labeled for (**A**) RyR2 (red) and (**B**) Na^+/Ca^{2+} exchange (NCX; red) with various Na^+ channel (Na$_v$) isoforms (Na$_v$1.x, green). These often resulted in an overlap between the immunofluorescent signals (yellow) when overlaid. (Right) Close-up views of regions highlighted by dashed white boxes. (Bottom) Representative fluorescent proximity ligation assay signal for RyR2 (**A**) and NCX (**B**) with different nNa$_v$ isoforms (Na$_v$1.x).

arrhythmogenic Ca^{2+} oscillations in WT cardiomyocytes exposed to isoproterenol (Figure 5B). This aberrant Ca^{2+} release resulted in a reduced SR Ca^{2+} load (Figure S4). Taken together, these data are consistent with the notion that enhanced nNa_v-mediated Na^+ influx is necessary as well as sufficient to produce proarrhythmic Ca^{2+} oscillations in WT atrial myocytes.

nNa_vs Modulate Atrial Arrhythmias in Mice

To determine the effects of nNa_v inhibition on atrial arrhythmias in mice with leaky RyR2,[32] we treated them with riluzole (15 mg/kg IP).[33] Atrial arrhythmia inducibility by atrial-burst pacing was reduced by half following riluzole treatment (Figure 6A). In contrast, augmentation of nNa_v-mediated Na^+ influx by β-pompilidotoxin (40 mg/kg IP) promoted atrial arrhythmias in WT mice: caffeine and epinephrine challenge induced atrial arrhythmias in 58% (7 of 12) of β-pompilidotoxin–treated mice, compared with 15% (2 of 13) of untreated controls (Figure 6B). Taken together, these data suggest that perturbing local Na^+-Ca^{2+} crosstalk via modulation of nNa_v potently regulates atrial arrhythmia risk in vivo.

Targeting nNa_vs With Riluzole Prevents Arrhythmias in a Canine Cardiomyopathy Model

Next, we examined the contribution of nNa_vs to atrial arrhythmogenesis in a clinically relevant chronic tachypacing-induced canine cardiomyopathy model (4 months of tachypacing).[4] This model allowed us to test the relevance of nNa_v blockade with riluzole in a much more complex pathology that goes beyond leaky RyR2. Riluzole (10 μmol/L) reduced the integral of persistent I_{Na}

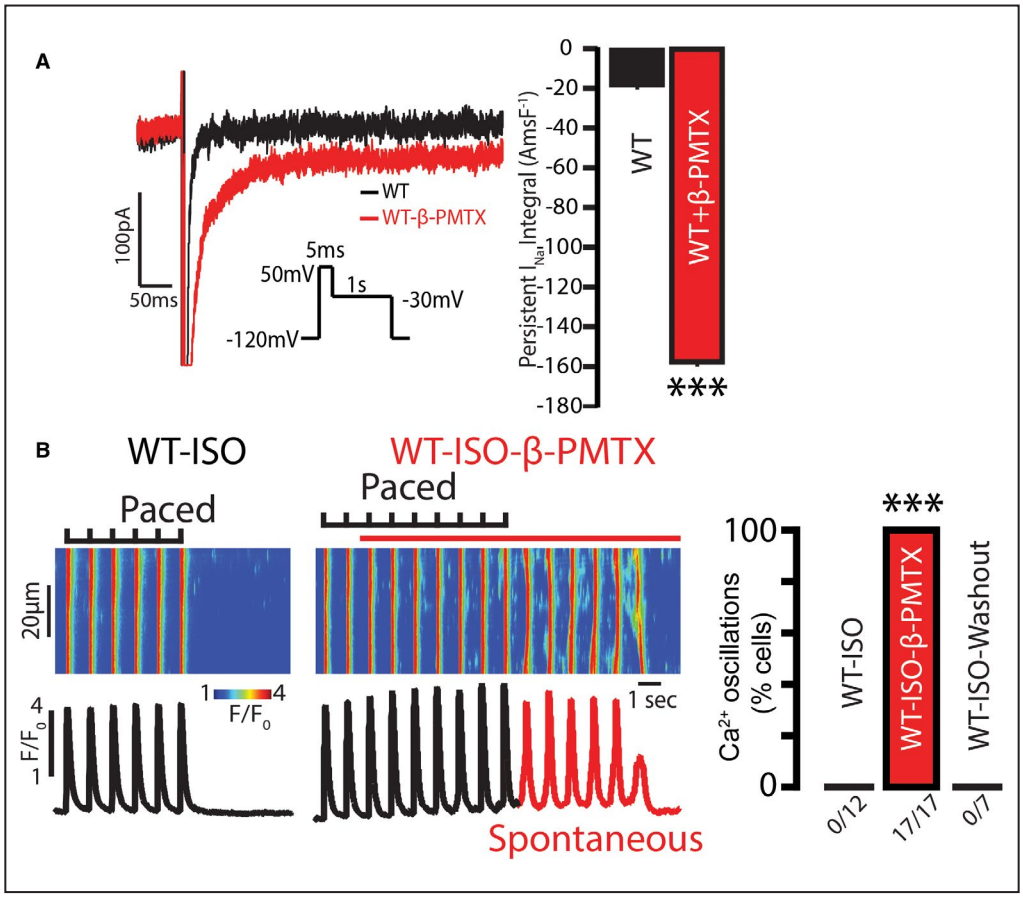

Figure 5. Augmentation of tetrodotoxin (TTX)-sensitive neuronal Na_v (nNa_v) is sufficient to initiate aberrant, repetitive Ca^{2+} oscillations in wild-type (WT) atrial myocytes.
A, Representative traces of persistent inward Na^+ currents (I_{Na}) recorded in WT atrial cardiomyocytes before (black) and after (red) exposure to β-pompilidotoxin (β-PMTX; 40 μmol/L). β-PMTX increased persistent I_{Na} relative to control (n=11 and 10 cells from 3 mice, respectively; ***P<0.0001 Wilcoxon rank sum test). **B**, (Left) Representative line scan images obtained from WT atrial cardiomyocytes exposed to isoproterenol (ISO; 100 nmol/L) and paced at 1 Hz. (Right) Rapid application of β-PMTX (40 μmol/L) induced aberrant, repetitive Ca^{2+} oscillations. (Median pacing frequency was 0.5 Hz with the range of 0.5 to 2 Hz; number of cells tested depicted under the corresponding bars, from N=3 mice; ***P<0.0001 Fisher exact test for ISO vs ISO–β-PMTX, ***P<0.0001 Fisher exact test for ISO–β-PMTX vs ISO-washout).

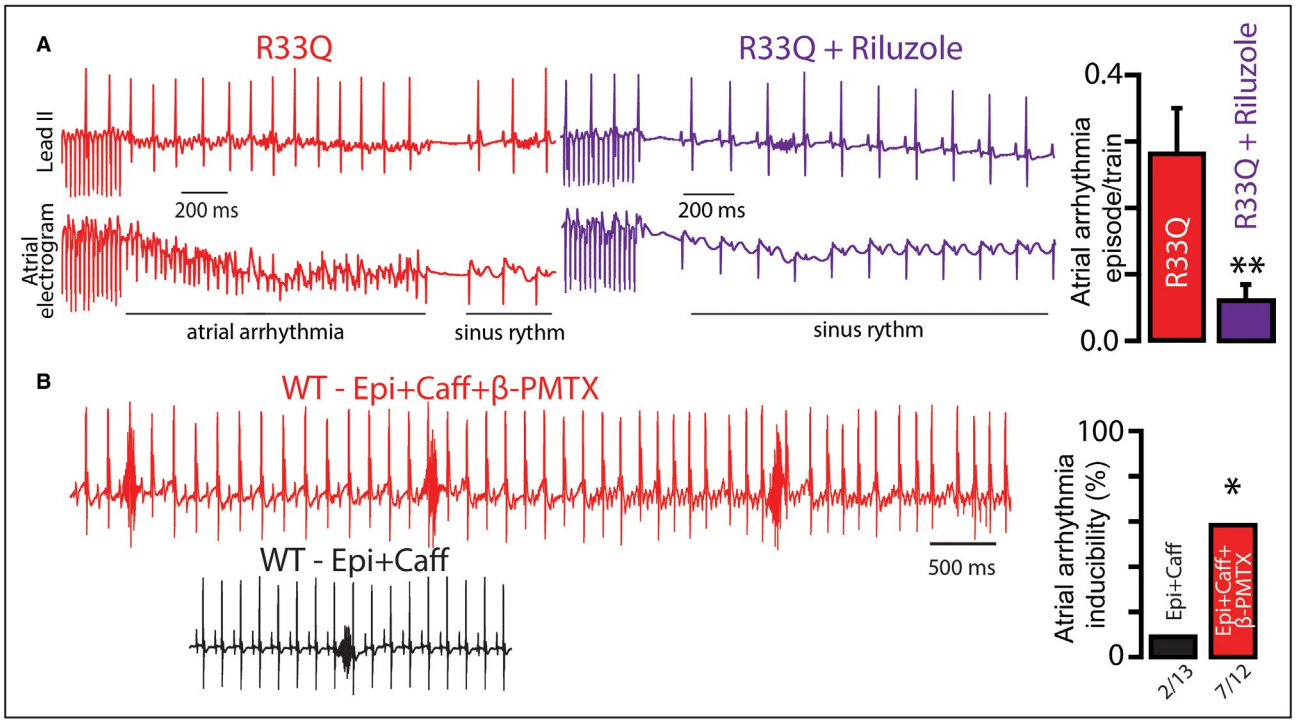

Figure 6. Modulation of tetrodotoxin (TTX)-sensitive neuronal Na_v (nNa_v) channel correspondingly modulates atrial arrhythmias in mice. **A**, Simultaneous surface ECG (lead II) and intracardiac atrial electrograms with frequent, rapid P waves and irregular RR intervals suggestive of atrial arrhythmia such as atrial flutter and atrial fibrillation in R33Q mice after burst pacing. Pretreatment with riluzole (Ril; 15 mg/kg IP), targeting plasma concentrations of ~10 μmol/L,[33] reduced the atrial arrhythmia inducibility (n=7 mice; ***P*=0.0160 Wilcoxon signed rank test). **B**, Representative surface ECG recordings of wild-type (WT) mice treated (top, red ECG) or untreated (bottom, black ECG) with β-pompilidotoxin (β-PMTX; 40 mg/kg IP) and exposed to catecholamine challenge with epinephrine (Epi, 1.5 mg/kg) and caffeine (Caff, 120 mg/kg). Since increased heart rate has been linked to reduced arrhythmia inducibility in calsequestrin null mice, and WT mice show higher heart rate relative to calsequestrin null mice,[32] all WT animals were pretreated with ivabradine (3 mg/kg) for 10 minutes before any intervention. Epi+Caff challenge during β-PMTX exposure precipitated repetitive P waves and irregular RR intervals suggestive of atrial arrhythmia in over 50% of WT mice, which is a 3-fold increase relative to β-PMTX–untreated mice (number of mice tested and those positive for atrial arrhythmias depicted under the corresponding bars; **P*=0.0410 Fisher exact test).

in the presence of isoproterenol (100 nmol/L) in nonfailing atria by 66±4%. This is consistent with the previous observation that about half of late I_{Na} in nonfailing canine ventricles is carried by tetrodotoxin-sensitive nNa_vs.[34] Atrial myocytes isolated from cardiomyopathic canines evidenced enhanced persistent I_{Na} at baseline, relative to controls (Figure 7A and 7B). In contrast to controls, isoproterenol (100 nmol/L) did not further enhance persistent I_{Na} in failing atrial cells (Figure 7A and 7B). In the context of increased post-translational modification of Ca^{2+} cycling proteins in this model,[4] these results may point to increased post-translational modification of Na_vs at baseline in failing hearts. Concurrently, proximity ligation assay revealed reduced incidence of $Na_v1.1$ and $Na_v1.3$ localizing in proximity to RyR2, while $Na_v1.6$ localization in proximity to both RyR2 and NCX was significantly increased (Figure S5). Importantly, riluzole (10 μmol/L) reduced the integral of persistent I_{Na} in failing myocytes to the same level as in nonfailing atria (–67±9 versus –74±13 Amp.ms/F for failing and nonfailing atria, respectively; Figure 7A and 7B). Notably, enhanced persistent I_{Na} integral in failing atrial myocytes translated into aberrant Ca^{2+} cycling: all isoproterenol-treated (100 nmol/L) failing atrial myocytes studied evidenced frequent, self-sustaining Ca^{2+} oscillations (Figure 7C and 7D). Riluzole (10 μmol/L) significantly reduced these events, an effect that was reversed upon washout (Figure 7C and 7D). Taken together, these data suggest the translatability of targeting nNa_vs with riluzole in complex pathologies.

Targeting nNa_vs With Riluzole Controls New-Onset AF in Patients With ALS

Based on the results from the canine model, we examined the effect of riluzole on atrial arrhythmias in human patients via a retrospective cohort study. The research cohort consisted of 184 Italian patients prescribed riluzole, 314 US patients prescribed riluzole, and 735 riluzole-free patients from the United States (Table). Compared with the no-riluzole patients, patients taking riluzole were age equivalent and had significantly more cardiovascular risk factors, more active

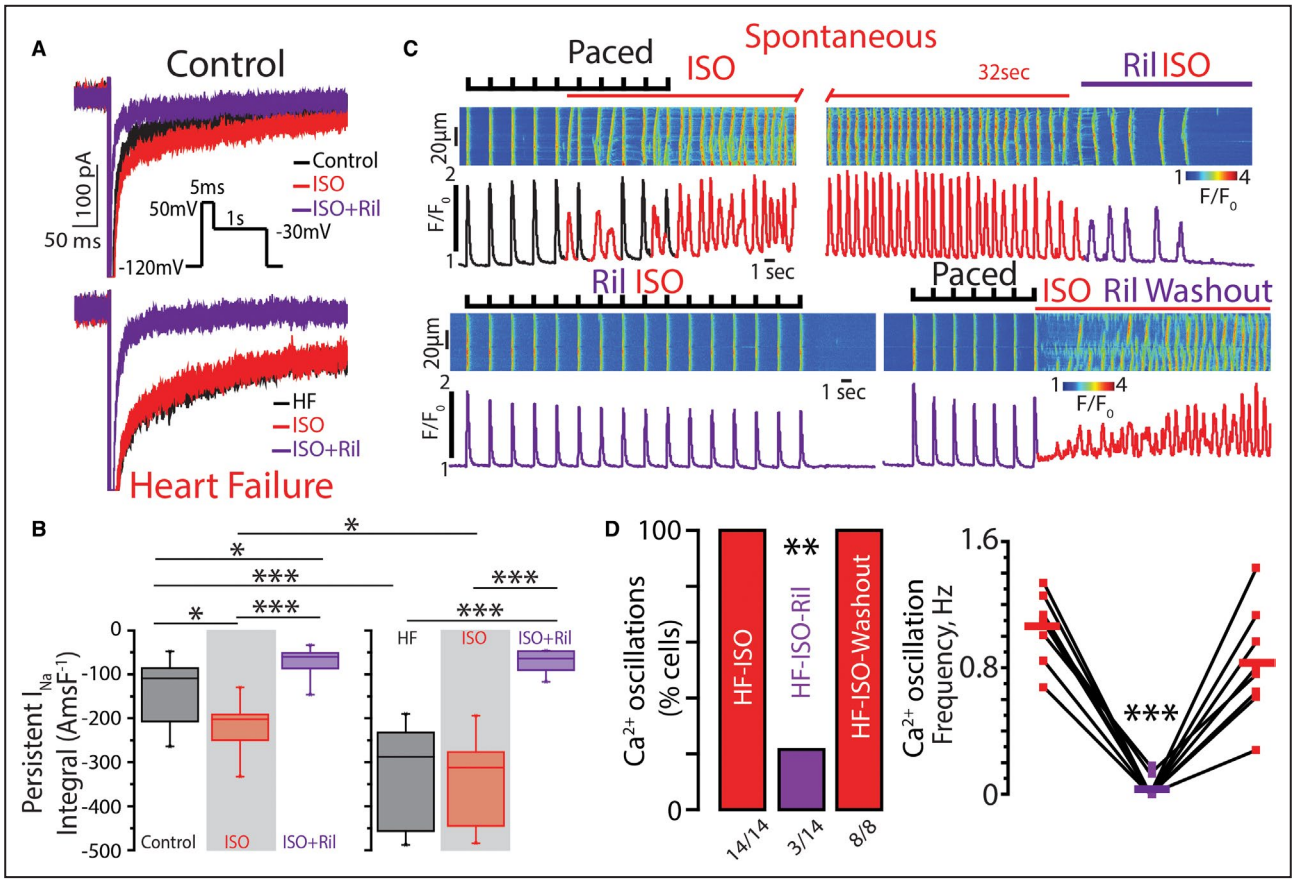

Figure 7. Riluzole (Ril) reduces enhanced, persistent inward Na⁺ currents (I_{Na}) and prevents induction of aberrant, repetitive Ca^{2+} oscillations in canine heart failure (HF) atrial myocytes.

A, Representative traces of persistent I_{Na} integral elicited using the protocol shown in the inset. Recordings were made in control (top) and failing (bottom) atrial myocytes before (black) and after exposure to isoproterenol (ISO; 100 nmol/L, red) and after treatment with Ril (10 µmol/L, purple). At baseline, atrial cardiomyocytes from failing hearts showed a larger persistent I_{Na} integral relative to control. ISO (100 nmol/L) enhanced persistent I_{Na} only in control cardiomyocytes. Ril reduced persistent I_{Na} integral in both control and failing atrial myocytes. **B**, Summary data are presented as persistent I_{Na} integral Amp-ms/F ($AmsF^{-1}$), which was measured by integrating I_{Na} between 50 and 450 ms (n=7 and 9 cells from 5 control and 3 failing dogs; $P<0.0001$ Kruskal–Wallis test; $^{*}P=0.0126$ for control vs ISO, $^{*}P=0.0209$ for control vs ISO+Ril, $^{*}P=0.0268$ for control-ISO vs HF-ISO, $^{***}P<0.0001$). **C**, Representative examples of the line-scan images and corresponding Ca^{2+} transients recorded in canine HF atrial cardiomyocytes loaded with Ca^{2+} indicator, Fluo-3 AM, and paced at 0.5 Hz with field stimulation. (Top) Cells were treated with ISO (100 nmol/L) and subsequently Ril (10 µmol/L; purple bar indicates time when Ril was added) was rapidly applied. (Bottom) Resumption of field stimulation failed to induce Ca^{2+} oscillations during concomitant exposure to ISO and Ril; however, washout of Ril resulted in their reinitiation. **D**, Ril significantly reduced the incidence of aberrant, repetitive Ca^{2+} oscillations, an effect that was washable (median pacing frequency was 0.5 Hz with the range of 0.5 to 1 Hz; number of cells tested depicted under the corresponding bars, N=3 animals for ISO and ISO-Ril, N=2 animals for ISO-washout, respectively; $^{**}P=0.0009$ McNemar test for ISO vs ISO-Ril, $P<0.0001$ Fisher exact test for ISO-Ril vs ISO-washout incidence; $^{***}P=0.0005$ Friedman rank sum test for Ca^{2+} oscillations frequency).

disease, and more recorded cardiovascular events. In addition, the riluzole cohort were prescribed significantly more cardiovascular risk prevention and treatment medications, including β-adrenergic blockers, Ca^{2+} channel blockers, aspirin, angiotensin system antagonists, and digitalis. The trends were consistent from both overall and US cohort analyses.

Patients with ALS treated with riluzole had significantly fewer overall cardiac arrhythmias. Five of 498 patients taking riluzole recorded tachyarrhythmia events versus 31 end points of 735 from the no-riluzole cohort over the maximum follow-up of 12 years, which resulted in the crude and adjusted HR of 0.28 (95% CI, 0.11–0.73; $P=0.0088$) and 0.25 (95% CI, 0.07–0.85; $P=0.0272$), respectively. The respective estimates when the analysis was limited to the US cohort were 0.25 (95% CI, 0.08–0.81; $P=0.0210$) and 0.21 (95% CI, 0.06–0.72; $P=0.0129$). The majority of arrhythmic events were distributed equivalently between supraventricular and ventricular tachycardia. The Kaplan–Meier curves of the arrhythmia events are presented in Figure 8, which reveals that arrhythmia events were reduced early and primarily throughout the first 2 years after riluzole

Table. Baseline Characteristics

	Riluzole, %		No Riluzole, %	Riluzole vs No Riluzole *P* Value	
	Italy and United States (n=501)	United States (n=314)	United States (n=735)	Overall Cohort	United States
Age ≥65 y	44.6	40.4	43.7	0.7475	0.3331
Concurrent conditions					
Hypertension	25.5	14.0	7.2	<0.0001	0.0005
Hyperlipidemia	12.1	6.4	2.9	<0.0001	0.0072
Diabetes mellitus	7.8	7.0	5.0	0.0481	0.2042
AMI or ACS	3.0	0.0	0.8	0.0036	0.1084
Active smoking	15.1	2.2	0.0	<0.0001	<0.0001
CAD	9.2	1.6	1.2	<0.0001	0.6344
HF	7.6	0.3	0.8	<0.0001	0.3644
Stroke	3.4	0.0	0.0	<0.0001	n/a
Current medication					
β-Blocker	6.6	0.3	0.0	<0.0001	0.1258
CCB	5.6	0.0	0.0	<0.0001	n/a
ASA	20.0	15.6	5.7	<0.0001	<0.0001
Statins	12.8	10.8	3.0	<0.0001	<0.0001
ACEI or ARB	20.8	11.1	2.3	<0.0001	<0.0001
Digitalis	0.8	0.0	0.0	0.0146	n/a

ACEI indicates angiotensin-converting enzyme inhibitor; ARB, angiotensin receptor blocker; ASA, acetyl salicylic acid (aspirin); CAD, coronary artery disease (other than acute myocardial infarction [AMI] or acute coronary syndrome [ACS]); CCB, calcium channel blocker; HF, heart failure; and n/a, not applicable.

prescribing. The majority of patients taking riluzole who recorded a tachyarrhythmia did not have cardiovascular disease. The rate of AF was lower in the rilozule group relative to the no-riluzole group (*P*=0.0492). Specifically, AF occurred in 22 patients with ALS: 13 from Italy and 9 from the United States. One AF event was recorded after the riluzole prescription versus 9 events from the no-riluzole cohort. Most patients who encountered AF had underlying cardiovascular disease (77%), with the majority treated with an angiotensin system antagonist; however, only 3 were treated with a β-adrenergic blocker.

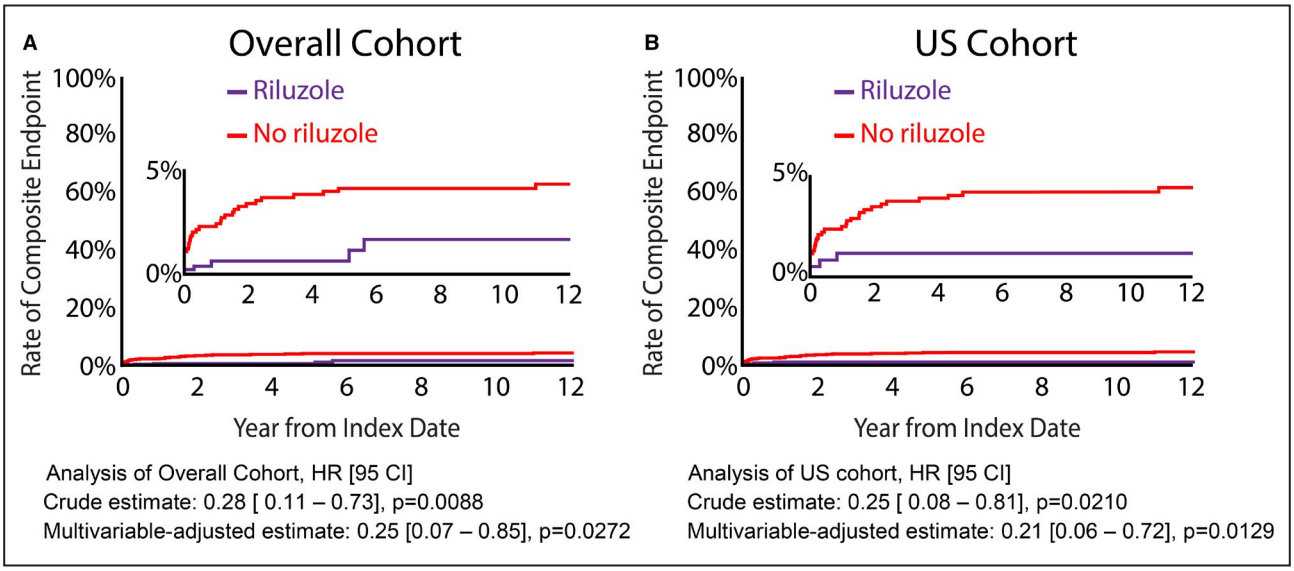

Figure 8. Riluzole prevents cardiac arrhythmias in patients with amyotrophic lateral sclerosis (ALS).
Two retrospective cohorts of ALS one exposed to riluzole vs no riluzole (controls), were compared by Cox proportional hazard models. The time-to-first composite arrhythmic events was analyzed using Kaplan–Meier production limit estimator. **A**, Overall cohort, (**B**) US cohort. HR indicates hazard ratio.

Riluzole safety was determined during the study period by recording any abnormal neutrophil count, or transaminase level (ie, alanine aminotransferase/serum glutamic pyruvic transaminase, aspartate aminotransferase/serum glutamic oxaloacetic transaminase, bilirubin, or gamma-glutamyl transferase levels). There was no record of any abnormal laboratory value in the study cohort.

DISCUSSION

AF is the most common sustained cardiac arrhythmia.[35] It is postulated that early use of rhythm control strategies may prevent arrhythmia progression.[36] Current antiarrhythmic drugs such as flecainide or amiodarone are moderately beneficial in restoration and maintenance of sinus rhythm but produce serious adverse effects such as ventricular tachycardia, negative inotropy, and extracardiac toxicity.[37,38] Therefore, there is a need for an effective and safe alternative to current antiarrhythmic therapy for AF. In this study, we have examined a nNa_V-mediated mechanism for atrial arrhythmias in various preclinical models. These studies identify nNa_Vs as a druggable target for safe and effective atrial arrhythmia prevention. To translate these results into a real-world setting, we undertook a retrospective cohort study of patients with ALS. Riluzole-treated patients with ALS had fewer AF and ventricular arrhythmias than those undergoing conventional ALS therapy without riluzole. Taken together, these findings suggest that riluzole merits serious consideration as treatment for atrial arrhythmias.

Role of nNa_Vs in Atrial Arrhythmias

Here, we demonstrate for the first time that nNa_Vs play a key role in the development of atrial arrhythmias in the presence of genetic (murine-CPVT; Figure 1) or acquired (canine-heart failure; Figure 7) Ca^{2+} handling dysfunction.[6,39] nNa_V blockade effectively suppressed atrial arrhythmias on the cellular level as well as in vivo (Figure 6). Contrariwise, acute experimental augmentation of nNa_V function was sufficient to precipitate cellular arrhythmias in healthy atrial myocytes (Figure 5). Further, augmentation of nNa_V activity reduced SR Ca^{2+} load (Figure S4), while inhibition of these channels had the opposite effect (Figure S1). This argues against global SR Ca^{2+} overload being the mechanism underlying the observed arrhythmias. Of note, blockade of other Na_V isoforms, including $Na_V1.5$, with R-propafenone[22–25] or ranolazine[26–29] in addition to nNa_Vs did not confer any apparent additional benefit beyond that achieved with 100 nmol/L of tetrodotoxin. This suggests that blockade of nNa_Vs is an important component of the antiarrhythmic mechanism of Na_V blockers.

Our structural results point to the close proximity of nNa_Vs to Ca^{2+}-handling machinery (RyR2 and NCX) as a potential factor underlying their privileged role in arrhythmogenesis (Figure 4 and Figure S5). In light of these findings, recent observations in patients with AF, which have revealed a reduction in $Na_V1.5$ and upregulation of nNa_Vs,[7] take on interesting implications. Mainly, remodeling within Na^+/Ca^{2+} nanodomain, composed of nNa_Vs and Ca^{2+}-handling machinery (Figure S5), may potentially compensate for failing excitation-contraction coupling. Inversely, the late I_{Na} carried by these channels (Figure 7A and 7B) and the consequent NCX, can facilitate aberrant Ca^{2+} release through sensitized leaky RyR2 (Figure 7C and 7D).[40,41] This is in line with other reports of increased nNa_V and enhanced late I_{Na} in failing rat, canine, and human hearts.[7,9,42] Hence, as proposed by our study, nNa_V blockade can be an effective antiarrhythmic strategy independent of remodeling within Na^+/Ca^{2+} nanodomain or the pathogenesis of leaky RyR2.[7,10,17,18,43] Furthermore, since ranolazine has been previously demonstrated to substantially affect multiple tetrodotoxin-sensitive and -resistant Na_V isoforms ($Na_V1.1$, $Na_V1.4$, $Na_V1.5$, $Na_V1.7$, and $Na_V1.8$)[26–28] at concentrations that are achieved therapeutically (<10 μmol/L), tetrodotoxin-sensitive nNa_V blockade may, in part, be an explanation for the effectiveness of ranolazine in reducing late I_{Na} in failing human atria.[7] However, despite our study pointing to nNa_Vs as antiarrhythmia targets, future research will need to determine the specific Na_V isoform, or the combination thereof, necessary for the antiarrhythmic effect of riluzole and other Na_V blockers, such as ranolazine. Taken together, these results indicate a direct role for nNa_V-mediated Na^+ influx in arrhythmia initiation, rather than it acting simply as a compounding factor.

Noteworthy, riluzole reduced persistent I_{Na} integral in nonfailing atria by 66±4%. This is consistent with previous observations that about half of late I_{Na} in canine ventricles is comprised of tetrodotoxin-sensitive nNa_Vs.[34] Furthermore, riluzole reduced persistent I_{Na} by similar absolute extents in both failing and nonfailing atrial myocytes. This corresponded to a greater proportional impact on persistent I_{Na} integral in failing myocytes (78±3%) versus nonfailing myocytes (66±4%) as a result of enhanced persistent I_{Na} in failing atria. Together, these data indicate a role for nNa_V remodeling within Ca^{2+}-handling nanodomains and increased post-translational modification of Na_Vs in failing atria. This notion is consistent with findings in atria from patients with chronic AF, where an increase in nNa_V isoforms accounted for increased late I_{Na} in AF.[7] However, despite the aforementioned studies providing a parallel to our results, we cannot rule out the potential involvement of $Na_V1.5$ in AF nor potential $Na_V1.5$ inhibition by riluzole to the drug's antiarrhythmic mechanism.

Riluzole-Treated Human Patients are Protected From AF

Whereas both tetrodotoxin and riluzole effectively suppressed atrial arrhythmias in animal models, concerns over toxicity render tetrodotoxin an untenable clinical option. In contrast, riluzole has a proven safety record as a treatment for ALS. In line with this, our data also suggest that riluzole was well tolerated. Hence, in our retrospective cohort study of arrhythmia risk among patients with ALS, riluzole-treated patients with ALS had both fewer AF and ventricular tachycardia diagnoses compared with nontreated patients (Figure 8). To our knowledge, this is the first evidence to show that riluzole may have antiarrhythmic properties in humans. However, because of the nonrandomized nature of this study, further controlled studies are necessary to confirm and extend this finding. Given that ventricular proarrhythmia is a critical limitation of current AF drug therapies,[13–15] riluzole and potentially other nNa_V inhibitors may provide an urgently needed safe alternative.

Limitations

A major limitation of small animal models is the translatability of findings into clinically relevant models of human disease. This factor is mitigated by our data demonstrating the antiarrhythmic efficacy of riluzole in a chronic tachypacing-induced canine cardiomyopathy model. Riluzole can activate small-conductance Ca^{2+}-activated K^+ channels,[44] which are upregulated in heart failure.[45] While the possible contribution of this effect to riluzole's antiarrhythmic mechanism is not clear, our results with other Na_V inhibitors suggest that it is not necessary. Whether small-conductance Ca^{2+}-activated K^+ channel activation contributes to riluzole's antiarrhythmic effect will be an interesting subject for future study. Na^+ channel blockers such as flecainide, R-propafenone, or ranolazine can block RyR2, mitigating the impact of leaky RyR2.[25,29,46] However, riluzole (10 µmol/L) did not affect Ca^{2+} sparks in permeabilized ventricular cardiomyocytes, a surrogate for RyR2 function.[17] Even so, this mechanism merits further study. It is important to note that our retrospective cohort study of patients with ALS helps translate findings from animal models to humans. However, the study's observational and nonrandomized nature offers limited insight into the causality of observed effects. This limitation was mitigated, in part, by adjusting outcomes for baseline characteristics. Finally, outcomes were retrospectively obtained and were only available from existing data; therefore, we were not able to include any arrhythmia observations outside of the databases. Since other studies demonstrated similar incidence of arrhythmias,[47] and valid results despite a similar limitation, we do not believe there would be differential ascertainment between the 2 cohorts.[48] However, because of the unique character of the population (ie, ALS), further controlled studies are necessary to confirm and extend our findings.

CONCLUSIONS

We used experimental and preclinical animal models to delineate a mechanistically driven therapeutic strategy for atrial arrhythmias and provide evidence for its translational potential from a community-based retrospective cohort. Specifically, we identify a nanodomain rich in nNa_Vs and Ca^{2+}-handling machinery (NCX and RyR2) that forms the basis of aberrant, self-sustained Ca^{2+} release, resulting in atrial arrhythmias in vivo. Importantly, inhibition of nNa_Vs with riluzole demonstrates efficacy in preventing atrial arrhythmias in both animal models and human patients. Thus, riluzole has the potential to be repurposed as a therapy for preventing AF.

ARTICLE INFORMATION

Received December 19, 2019; accepted April 24, 2020.

Affiliations

From the Departments of Pharmacotherapy and Internal Medicine (M.A.M.) and Pharmacotherapy (K.K., J.B.), University of Utah Health Sciences Center, Salt Lake City, UT; Dorothy M. Davis Heart and Lung Research Institute, College of Medicine, The Ohio State University Wexner Medical Center, Columbus, OH (Y.O., M.L.K., Q.L., I.B., C.A.C., R.V., S.G., P.B.R.); Division of Pharmacy Practice and Sciences, College of Pharmacy (Y.O., M.L.K., C.A.C., P.B.R.), Department of Physiology and Cell Biology, College of Medicine (Q.L., I.B., S.G., R.V., P.B.R.), and Department of Biomedical Engineering, College of Engineering (H.L.S., R.V.), The Ohio State University, Columbus, OH; Department of Neuroscience, St. Agostino Estense Hospital, Azienda Ospedaliero Universitaria di Modena, Italy (J.M.); Department of Internal Medicine and of Molecular & Integrative Physiology, University of Michigan, Ann Arbor, MI (R.R.M., H.H.V.); Molecular Cardiology, Istituti Clinici Scientifici Maugeri, IRCCS (S.G.P.) and Department of Molecular Medicine (S.G.P.), University of Pavia, Italy; Department of Biomedical Sciences, University of Padova, Italy (P.V.).

Acknowledgments

Munger and Radwański provided conception/design of the work; Munger, Olğar, Koleske, Struckman, Mandrioli, Lou, Bonila, Kim, Ramos Mondragon, and Radwański performed research; Priori, Volpe, Biskupiak, Valdivia, and Carnes contributed tools; Olğar, Koleske, Struckman, Kim, Ramos Mondragon, Veeraraghavan, and Radwański analyzed data; and Munger, Veeraraghavan, Györke, and Radwański drafted the work or revised it critically for important intellectual content.

Sources of Funding

This work was supported by National Institutes of Health grants HL074045, HL063043 (to Györke), and HL127299 (to Radwański), as well as a Saving tiny Hearts grant and American Heart Association 19TPA34910191 (to Radwański).

Disclosures

Kim reports research grants from AstraZeneca, Myriad Genetics, and Pacira Pharmaceuticals. The remaining authors have no disclosures to report.

Supplementary Materials

Data S1
Figures S1–S5
References 49–51

REFERENCES

1. Miyasaka Y, Barnes ME, Gersh BJ, Cha SS, Bailey KR, Abhayaratna WP, Seward JB, Tsang TSM. Secular trends in incidence of atrial fibrillation in Olmsted County, Minnesota, 1980 to 2000, and implications on the projections for future prevalence. *Circulation*. 2006;114:119–125.
2. Bhuiyan ZA, van den Berg MP, van Tintelen JP, Bink-Boelkens MT, Wiesfeld AC, Alders M, Postma AV, van Langen I, Mannens MM, Wilde AA. Expanding spectrum of human RYR2-related disease: new electrocardiographic, structural, and genetic features. *Circulation*. 2007;116:1569–1576.
3. Lubitz SA, Benjamin EJ, Ellinor PT. Atrial fibrillation in congestive heart failure. *Heart Fail Clin*. 2010;6:187–200.
4. Belevych AE, Terentyev D, Terentyeva R, Nishijima Y, Sridhar A, Hamlin RL, Carnes CA, Györke S. The relationship between arrhythmogenesis and impaired contractility in heart failure: role of altered ryanodine receptor function. *Cardiovasc Res*. 2011;90:493–502.
5. Heijman J, Wehrens XH, Dobrev D. Atrial arrhythmogenesis in catecholaminergic polymorphic ventricular tachycardia–is there a mechanistic link between sarcoplasmic reticulum Ca(2+) leak and re-entry? *Acta Physiol (Oxf)*. 2013;207:208–211.
6. Lou Q, Belevych AE, Radwański PB, Liu B, Kalyanasundaram A, Knollmann BC, Fedorov VV, Györke S. Alternating membrane potential/calcium interplay underlies repetitive focal activity in a genetic model of calcium-dependent atrial arrhythmias. *J Physiol*. 2015;593:1443–1458.
7. Sossalla S, Kallmeyer B, Wagner S, Mazur M, Maurer U, Toischer K, Schmitto JD, Seipelt R, Schöndube FA, Hasenfuss G, et al. Altered Na(+) currents in atrial fibrillation effects of ranolazine on arrhythmias and contractility in human atrial myocardium. *J Am Coll Cardiol*. 2010;55:2330–2342.
8. Zicha S, Maltsev VA, Nattel S, Sabbah HN, Undrovinas AI. Post-transcriptional alterations in the expression of cardiac Na^+ channel subunits in chronic heart failure. *J Mol Cell Cardiol*. 2004;37:91–100.
9. Mishra S, Reznikov V, Maltsev VA, Undrovinas NA, Sabbah HN, Undrovinas A. Contribution of sodium channel neuronal isoform Nav1.1 to late sodium current in ventricular myocytes from failing hearts. *J Physiol*. 2015;593:1409–1427.
10. Radwański PB, Ho HT, Veeraraghavan R, Brunello L, Liu B, Belevych AE, Unudurthi SD, Makara MA, Priori SG, Volpe P, et al. Neuronal Na^+ channels are integral components of pro-arrhythmic Na^+/Ca^{2+} signaling nanodomain that promotes cardiac arrhythmias during β-adrenergic stimulation. *JACC Basic Transl Sci*. 2016;1:251–266.
11. Radwański PB, Poelzing S. NCX is an important determinant for premature ventricular activity in a drug-induced model of Andersen-Tawil syndrome. *Cardiovasc Res*. 2011;92:57–66.
12. Radwański PB, Veeraraghavan R, Poelzing S. Cytosolic calcium accumulation and delayed repolarization associated with ventricular arrhythmias in a guinea pig model of Andersen-Tawil syndrome. *Heart Rhythm*. 2010;7:1428–1435.
13. Preliminary report: effect of encainide and flecainide on mortality in a randomized trial of arrhythmia suppression after myocardial infarction. The Cardiac Arrhythmia Suppression Trial (CAST) Investigators. *N Engl J Med*. 1989;321:406–412.
14. Starmer CF, Lastra AA, Nesterenko VV, Grant AO. Proarrhythmic response to sodium channel blockade. Theoretical model and numerical experiments. *Circulation*. 1991;84:1364–1377.
15. Hohnloser SH, Singh BN. Proarrhythmia with class III antiarrhythmic drugs: definition, electrophysiologic mechanisms, incidence, predisposing factors, and clinical implications. *J Cardiovasc Electrophysiol*. 1995;6:920–936.
16. Song JH, Huang CS, Nagata K, Yeh JZ, Narahashi T. Differential action of riluzole on tetrodotoxin-sensitive and tetrodotoxin-resistant sodium channels. *J Pharmacol Exp Ther*. 1997;282:707–714.
17. Radwański PB, Brunello L, Veeraraghavan R, Ho HT, Lou Q, Makara MA, Belevych AE, Anghelescu M, Priori SG, Volpe P, et al. Neuronal Na^+ channel blockade suppresses arrhythmogenic diastolic Ca^{2+} release. *Cardiovasc Res*. 2015;106:143–152.
18. Koleske M, Bonilla I, Thomas J, Zaman N, Baine S, Knollmann BC, Veeraraghavan R, Györke S, Radwański PB. Tetrodotoxin-sensitive Na_vs contribute to early and delayed afterdepolarizations in long QT arrhythmia models. *J Gen Physiol*. 2018;150:991–1002.
19. Weiss S, Benoist D, White E, Teng W, Saint DA. Riluzole protects against cardiac ischaemia and reperfusion damage via block of the persistent sodium current. *Br J Pharmacol*. 2010;160:1072–1082.
20. Lacomblez L, Bensimon G, Leigh PN, Debove C, Bejuit R, Truffinet P, Meininger V; ALS Study Groups I and II. Long-term safety of riluzole in amyotrophic lateral sclerosis. *Amyotroph Lateral Scler Other Motor Neuron Disord*. 2002;3:23–29.
21. Bensimon G, Lacomblez L, Meininger V. A controlled trial of riluzole in amyotrophic lateral sclerosis. ALS/Riluzole Study Group. *N Engl J Med*. 1994;330:585–591.
22. Edrich T, Wang SY, Wang GK. State-dependent block of human cardiac hNav1.5 sodium channels by propafenone. *J Membr Biol*. 2005;207:35–43.
23. Desaphy JF, Carbonara R, Costanza T, Conte Camerino D. Preclinical evaluation of marketed sodium channel blockers in a rat model of myotonia discloses promising antimyotonic drugs. *Exp Neurol*. 2014;255:96–102.
24. Bang S, Yoo J, Gong X, Liu D, Han Q, Luo X, Chang W, Chen G, Im S-T, Kim YH, et al. Differential Inhibition of Nav1.7 and neuropathic pain by hybridoma-produced and recombinant monoclonal antibodies that target Nav1.7. *Neurosci Bull*. 2018;34:22–41.
25. Faggioni M, Savio-Galimberti E, Venkataraman R, Hwang HS, Kannankeril PJ, Darbar D, Knollmann BC. Suppression of spontaneous Ca elevations prevents atrial fibrillation in calsequestrin 2-null hearts. *Circ Arrhythm Electrophysiol*. 2014;7:313–320.
26. Wang GK, Calderon J, Wang SY. State- and use-dependent block of muscle Nav1.4 and neuronal Nav1.7 voltage-gated Na^+ channel isoforms by ranolazine. *Mol Pharmacol*. 2008;73:940–948.
27. Kahlig KM, Hirakawa R, Liu L, George AL, Belardinelli L, Rajamani S. Ranolazine reduces neuronal excitability by interacting with inactivated states of brain sodium channels. *Mol Pharmacol*. 2014;85:162–174.
28. Rajamani S, Shryock JC, Belardinelli L. Block of tetrodotoxin-sensitive, Na(V)1.7 and tetrodotoxin-resistant, Na(V)1.8, Na^+ channels by ranolazine. *Channels (Austin)*. 2008;2:449–460.
29. Parikh A, Mantravadi R, Kozhevnikov D, Roche MA, Ye Y, Owen LJ, Puglisi JL, Abramson JJ, Salama G. Ranolazine stabilizes cardiac ryanodine receptors: a novel mechanism for the suppression of early afterdepolarization and Torsades de Pointes in long QT type 2. *Heart Rhythm*. 2012;9:953–960.
30. Rhett JM, Ongstad EL, Jourdan J, Gourdie RG. Cx43 associates with Na(v)1.5 in the cardiomyocyte perinexus. *J Membr Biol*. 2012;245:411–422.
31. Schiavon E, Stevens M, Zaharenko AJ, Konno K, Tytgat J, Wanke E. Voltage-gated sodium channel isoform-specific effects of pompilidotoxins. *FEBS J*. 2010;277:918–930.
32. Faggioni M, Hwang HS, van der Werf C, Nederend I, Kannankeril PJ, Wilde AA, Knollmann BC. Accelerated sinus rhythm prevents catecholaminergic polymorphic ventricular tachycardia in mice and in patients. *Circ Res*. 2013;112:689–697.
33. Milane A, Tortolano L, Fernandez C, Bensimon G, Meininger V, Farinotti R. Brain and plasma riluzole pharmacokinetics: effect of minocycline combination. *J Pharm Pharm Sci*. 2009;12:209–217.
34. Biet M, Barajas-Martínez H, Ton AT, Delabre JF, Morin N, Dumaine R. About half of the late sodium current in cardiac myocytes from dog ventricle is due to non-cardiac-type Na(+) channels. *J Mol Cell Cardiol*. 2012;53:593–598.
35. Chugh SS, Havmoeller R, Narayanan K, Singh D, Rienstra M, Benjamin EJ, Gillum RF, Kim YH, McAnulty JH, Zheng ZJ, et al. Worldwide epidemiology of atrial fibrillation: a Global Burden of Disease 2010 Study. *Circulation*. 2014;129:837–847.
36. Camm AJ, Dorian P, Hohnloser SH, Kowey PR, Tyl B, Ni Y, Vandzhura V, Maison-Blanche P, de Melis M, Sanders P. A randomized, double-blind, placebo-controlled trial assessing the efficacy of S66913 in patients with paroxysmal atrial fibrillation. *Eur Heart J Cardiovasc Pharmacother*. 2019;5:21–28.
37. Tamargo J, Caballero R, Gómez R, Delpón E. I(Kur)/Kv1.5 channel blockers for the treatment of atrial fibrillation. *Expert Opin Investig Drugs*. 2009;18:399–416.
38. Lau W, Newman D, Dorian P. Can antiarrhythmic agents be selected based on mechanism of action? *Drugs*. 2000;60:1315–1328.
39. Glukhov AV, Kalyanasundaram A, Lou Q, Hage LT, Hansen BJ, Belevych AE, Mohler PJ, Knollmann BC, Periasamy M, Györke S, et al. Calsequestrin 2 deletion causes sinoatrial node dysfunction and atrial arrhythmias associated with altered sarcoplasmic reticulum calcium cycling and degenerative fibrosis within the mouse atrial pacemaker complex. *Eur Heart J*. 2015;36:686–697.
40. Radwański PB, Johnson CN, Györke S, Veeraraghavan R. Cardiac arrhythmias as manifestations of nanopathies: an emerging view. *Front Physiol*. 2018;9:1228.

41. Veeraraghavan R, Györke S, Radwański PB. Neuronal sodium channels: emerging components of the nano-machinery of cardiac calcium cycling. *J Physiol*. 2017;595:3823–3834.
42. Xi Y, Wu G, Yang L, Han K, Du Y, Wang T, Lei X, Bai X, Ma A. Increased late sodium currents are related to transcription of neuronal isoforms in a pressure-overload model. *Eur J Heart Fail*. 2009;11:749–757.
43. Radwański PB, Greer-Short A, Poelzing S. Inhibition of Na^+ channels ameliorates arrhythmias in a drug-induced model of Andersen-Tawil syndrome. *Heart Rhythm*. 2013;10:255–263.
44. Dimitriadi M, Kye MJ, Kalloo G, Yersak JM, Sahin M, Hart AC. The neuroprotective drug riluzole acts via small conductance Ca^{2+}-activated K^+ channels to ameliorate defects in spinal muscular atrophy models. *J Neurosci*. 2013;33:6557–6562.
45. Chang PC, Chen PS. SK channels and ventricular arrhythmias in heart failure. *Trends Cardiovasc Med*. 2015;25:508–514.
46. Watanabe H, Chopra N, Laver D, Hwang HS, Davies SS, Roach DE, Duff HJ, Roden DM, Wilde AA, Knollmann BC. Flecainide prevents catecholaminergic polymorphic ventricular tachycardia in mice and humans. *Nat Med*. 2009;15:380–383.
47. Scirica BM, Morrow DA, Hod H, Murphy SA, Belardinelli L, Hedgepeth CM, Molhoek P, Verheugt FW, Gersh BJ, McCabe CH, et al. Effect of ranolazine, an antianginal agent with novel electrophysiological properties, on the incidence of arrhythmias in patients with non ST-segment elevation acute coronary syndrome: results from the Metabolic Efficiency with Ranolazine for Less Ischemia in Non ST-Elevation Acute Coronary Syndrome Thrombolysis in Myocardial Infarction 36 (MERLIN-TIMI 36) randomized controlled trial. *Circulation*. 2007;116:1647–1652.
48. Mortensen EM, Halm EA, Pugh MJ, Copeland LA, Metersky M, Fine MJ, Johnson CS, Alvarez CA, Frei CR, Good C, et al. Association of azithromycin with mortality and cardiovascular events among older patients hospitalized with pneumonia. *JAMA*. 2014;311:2199–2208.
49. Nishijima Y, Feldman DS, Bonagura JD, Ozkanlar Y, Jenkins PJ, Lacombe VA, Abraham WT, Hamlin RL, Carnes CA. Canine nonischemic left ventricular dysfunction: a model of chronic human cardiomyopathy. *J Card Fail*. 2005;11:638–644.
50. Belevych AE, Ho HT, Bonilla IM, Terentyeva R, Schober KE, Terentyev D, Carnes CA, Györke S. The role of spatial organization of Ca^{2+} release sites in the generation of arrhythmogenic diastolic Ca^{2+} release in myocytes from failing hearts. *Basic Res Cardiol*. 2017;112:44.
51. Bao Y, Willis BC, Frasier CR, Lopez-Santiago LF, Lin X, Ramos-Mondragón R, Auerbach DS, Chen C, Wang Z, Anumonwo J, et al. Scn2b deletion in mice results in ventricular and atrial arrhythmias. *Circ Arrhythm Electrophysiol*. 2016;9:e003923.

Supplemental Materials

Data S1. Methods

Canine model of heart failure

Ventricular dysfunction was induced by right ventricular tachypacing, as described previously.[49] Briefly, adult hound dogs (17–31 kg) of either sex were chronically instrumented with modified pacemakers (St. Jude Medical, MN) with the pacing lead (St. Jude Medical, MN) placed in the right ventricle apex. Tachypacing was performed at: 180 bpm for 2 weeks, 200 bpm for 6 weeks, and 180 bpm thereafter. This tachypacing protocol induced HF in these dogs as evidenced by LV dysfunction, and functional impairment, which was reported in Belevych et al.[50] Cellular studies were performed following 16 weeks of tachypacing unless otherwise stated.

Myocyte isolation, confocal Ca^{2+} imaging Na^{+} current recordings

The dogs were anesthetized with pentobarbital sodium (50 mg/kg intravenously; Nembutal, Abbott Laboratories, IL), and the heart was rapidly removed and perfused with ice-cold cardioplegic solution containing the following (mM): NaCl 110, $CaCl_2$ 1.2, KCl 16, $MgCl_2$ 16, and $NaHCO_3$ 10. Left circumflex artery was cannulated and used to perfuse both the left atria and left ventricle. The heart was perfused for 10 min with a perfusion buffer containing (mM) NaCl 130, KCl 5.4, $MgCl_2$ 3.5, NaH_2PO_4 0.5, Glucose 10, HEPES 5, and taurine 20 supplemented with 0.1 mM EGTA; this was followed by heart perfusion with the perfusion buffer containing 0.3 mM Ca^{2+}, 0.12 mg/ml of soybean trypsin inhibitor (Thermo Fisher Scientific, MA), and 1.33 mg/ml of type II collagenase (lot number 44C14804B, activity 265 U/mg, Worthington Biochemical Corp, NJ) for 30 min. Following enzymatic digestion, left atrial appendage was dissected and

placed in shaking water bath at 37° C for additional 10 min. Murine atrial myocytes were obtained by enzymatic isolation from 3-11 month old cardiac calsequestrin mutant (R33Q) mice (on C57BL/6 background)[18] as well as wild type (WT; on C57BL/6 background obtained from Jackson Labs, ME) mice of both genders. Mice were anaesthetized with isoflurane and once a deep level of anaesthesia was reached, the hearts were rapidly removed and Langendorff perfused as previously described [10,17,18].

Whole-cell patch clamp recordings of late and peak sodium currents (I_{Na}) were recorded using internal solution containing in mM: 10 NaCl, 20 TEACl, 123 CsCl, 1 $MgCl_2$, 0.1 Tris GTP, 5 MgATP, 10 HEPES, 1 EGTA while free Ca^{2+} was maintained at 100 nmol/L with $CaCl_2$ (pH 7.2).[10,18] The extracellular bathing solution for late I_{Na} recordings contained in mM: 140 NaCl, 4 CsCl, 1 $CaCl_2$, 2 $MgCl_2$, 0.05 $CdCl_2$, 10 HEPES, 10 glucose, 0.03 niflumic acid, 0.004 strophanthidin and 0.2 $NiCl_2$. pH was maintained at 7.4 with CsOH. For peak I_{Na} recordings, extracellular bathing solution was altered by reducing NaCl to 10 mM, CsCl was increased to 123 mM and 20 mM TEACl was added. Whole-cell capacitance and series resistance compensation (≥60%) was applied along with leak subtraction. Signals were filtered with 10 kHz Bessel filter and I_{Na} was then normalized to membrane capacitance. Late I_{Na} was measured as the current integral from 50 to 450 ms from the beginning of the pulse, unless otherwise stated.[18]

Intracellular Ca^{2+} cycling was monitored by either Nikon A1R HD or Olympus FluoView 1000 laser scanning confocal microscopes equipped with 60x 1.4 NA oil objectives. For intact, field-stimulated myocytes, we used the cytosolic Ca^{2+}-sensitive indicators Fluo-3

AM (Molecular Probes, Eugene, OR). Cells were electrically stimulated between 0.5 and 7 Hz using extracellular platinum electrodes at lowest frequency necessary to induce Ca^{2+} oscillation in the presence of isopreteranol (100 nM; Sigma, St. Louis, MO) and/or tetrodotoxin (100 nM; Tocris Bioscience, UK), riluzole (10 μM; Sigma, St. Louis, MO), ranolazine (10 μM; Sigma, St. Louis, MO), or R-propafenone (300 nM; Santa Cruz, Dallas, TX). To assess SR Ca^{2+} load cells were paced at 0.5 Hz for at least 10 sec. and 20 mM caffeine (Sigma, St. Louis, MO) was rapidly applied. The fluorescent probes were excited with the 488 nm line of an argon laser and emission was collected at 500–600 nm. The fluorescence emitted was expressed as F/F_0, where F is the fluorescence at time t and F_0 represents the background signal. All experiments were performed at room temperature (26°C).

Intracardiac Recording

Following the achievement of surgical anesthesia, with isoflurane (1-1.5%), an octapolar catheter (iWorx Science, Dover, NH) was inserted through the jugular vein and advanced into the right atrium and ventricle. Arrhythmia inducibility was assessed by the application of 12 to 18 atrial bursts of pacing (50 HZ for 2 or 5 sec) as previously described.[51] If no arrhythmia was observed under control conditions intraperitoneal carbachol (50 ng/g; Sigam, St. Louis, MO) was administrated (2 vs. 5 mice, respectively). Mice with long-lasting AF episodes after carbachol administration were excluded from the analysis. Atrial bursts of pacing was then repeated after intraperitoneal riluzole (15 mg/kg; Sigam, St. Louis, MO) administration. AF was defined

as the occurrence of rapid and fragmented atrial electrograms (lack of regular P waves) with irregular AV nodal conduction and ventricular rhythm, all lasting at least 1 s.[51]

Surface electrocardiographic recordings

Continuous electrocardiographic (ECG) recordings (PL3504 PowerLab 4/35, ADInstruments; Colorado Springs, CO) were obtained from mice anesthetized with isoflurane (1-1.5%) as previously described [10,17,18]. Since increased heart rate has been linked to reduced arrhythmia inducibility in CPVT, and WT mice evidence higher HR relative to CPVT [32], all WT animals were pretreated with ivabradine (3 mg/kg, Sigma , St. Louis, MO) for 10 min. before any intervention. After baseline recording (5 min.) and ivabradine (10 min.), animals received either intraperitoneal β-Pompilidotoxin (β-PMTX; 40 mg/kg; Alomone Labs, Israel) or no therapy. After additional 5-10 min animals were exposed to an intraperitoneal epinephrine (1.5 mg/kg; Sigma, St. Louis, MO) and caffeine (120 mg/kg; Sigma, St. Louis, MO) challenge and ECG recording continued for 20 mins. ECG recordings were analyzed using the LabChart 7.3 program (ADInstruments; Colorado Springs, CO).

Immunofluorescent labeling of myocytes

Isolated atrial myocytes were prepared for immunofluorescence as well as proximity ligation assay (PLA) as described previously.[10] Briefly, cells were plated on laminin-coated glass coverslips, fixed with 4% paraformaldehyde for 5 min, permeabilized with 0.1% Triton X-100, and washed with PBS. Endogenous immunoglobulin was blocked using a 2% BSA PBS solution for 1 h at room temperature and subsequently incubated

with primary antibodies. We immunolabled for nNa_vs (Na_v1.1, 1.3, 1.6; Alomone, Jerusalem, Israel), NCX (Thermo Scientific, Rockford, IL, USA) and for RyR2 (Pierce Antibodies, Rockford, IL, USA.) overnight at 4°C. For immunofluorescence after washing, goat secondary antibodies (anti-mouse and anti-rabbit) conjugated to Alexa Fluor 488 or 549 (Life Technologies, Grand Island, NY, USA) were added for 1 h. While the PLA reactions were carried out using appropriate Duolink (Sigma, St. Louise, MO, USA) secondary antibodies according to the manufacturer's instructions.

Retrospective Cohort Study Population

This was a population-based, retrospective cohort study of patients with amyotrophic lateral sclerosis (ALS) who were either treated with riluzole (study group) versus no riluzole (control group) from the ALS Centre of the Azienda Ospedaliero, Universitaria di Modena, Modena, Italy, and Enterprise Data Warehouse, University of Utah, Salt Lake City, Utah, USA. Both databases contained all electronic health record data, including clinical, laboratory, and administrative data for all patients. Both contained structural electronic health records including clinical, laboratory, and administrative data for all patients. Patients in the exposure group had one or more records of riluzole prescriptions. Patients having a history of ALS diagnosis without a record of riluzole were eligible for the control group. The U.S. Food and Drug Administration indication for riluzole is for the treatment of patients with ALS. Because of this limited indication, only ALS patients were studied to determine whether riluzole would prevent tachyarrhythmias.

Clinical record databases were searched for based on code 335.2 (ALS) of the *International Classification of Diseases* (9th revision,; ICD-9-CM). Study data for Italy were collected from December, 31st, 1989 through June 30th, 2017 and for the U.S. data was February 3rd, 1998 through June 30th, 2017. Index date for the exposure group was the date of the first prescription for riluzole. For the control group, index date was the earliest available date from the data on or after the diagnosis of ALS.

All patients were included if they were at least 18 years old (with no upper age cutoff). Arrhythmia was defined using Current Procedural Terminology (CPT) and International Classification of Diseases, Ninth or Tenth Revisions, Clinical Modification (ICD-9-CM) or (ICD-10-CM) codes: 427.1/147.9 paroxysmal ventricular tachycardia, 427.0/147.1, cardiac arrhythmia, unspecified 427.9/149.9, paroxysmal supraventricular tachycardia, or atrial fibrillation 427.31/148.0/148.91. Patients were censored at their date of death if they died during the study period.

Data was collected through queries of structured data fields. Variables extracted from structured fields included patient demographic variables (i.e., age on the index date, sex, race, and BMI), laboratory results, diagnostic tests and results, all medication prescriptions, hospitalizations for cardiovascular causes including acute coronary syndrome, acute myocardial infarction, heart failure and any arrhythmia including atrial flutter or fibrillation. Race and ethnicity categories included White, Black, Hispanic, Asian, and other/unknown. Cardiovascular risk factors and specific medications for cardiovascular risk prevention and treatment were collected and identified.

Characteristics of the study population were calculated among the overall population, Italy and USA databases, and among riluzole versus no riluzole users. Cardiac pacemaker and implantable cardio-defibrillator placement were collected, if applicable.

The primary outcomes were the difference the occurrence of any arrhythmia and atrial fibrillation between the riluzole and no riluzole cohorts. The primary analyses followed intention-to-treat principles (i.e., post-index date variables were not incorporated into the analysis such as medication adherence). All tests were 2-tailed with an alpha of 0.05 for statistical significance. All data were analyzed with SAS v9.4 (Cary, NC) with significance set at a *p*-value set at <0.05.

Data analysis

For the population-based, retrospective cohort study descriptive analyses were used to compare baseline characteristics (i.e., patient-level characteristics at the index date) between the exposure and control groups. Age distributions were compared using a student t-test, and categorical variables including demographic information other than age, history of specific cardiovascular conditions and medication indicated for the cardiovascular conditions using Chi-square tests. A Fisher's exact test replaced Chi-square test when the expected number of patients in a cell of a frequency table was less than 5. Comparing baseline characteristics was performed between the two healthcare settings, Italy and Utah.

The analysis of outcomes followed intention-to-treat principles (i.e., post-index date variables such as medication adherence, discontinuation or new onset of another cardiovascular conditions were not incorporated into the analysis). Time to first composite arrhythmic events and AF events were analyzed using a Kaplan-Meier product limit estimator. Patients follow-up continued until a patient encountered with the outcome of interest, end of the data collection period (i.e., June 30th, 2017), 11 years (4,018 days) after the index date or date of death, whichever came first. The analytic follow-up timeline was determined based on the latest arrhythmic event eligible for the study endpoint which incurred at 4,010 days (10.98 years) after the index date. Thereafter no additional failure would be seen on the Kaplan-Meier curves.

The hazard ratios (HRs) of the outcomes for the exposure vs. control were estimated using Cox-proportional hazard models. Initial study plan proposed the exposure-outcome association adjusted for potential confounders which were selected based on baseline characteristics where the p-value in the comparison was less than 0.1. Statistical significance was determined from a 2-tailed test with an alpha of 0.05. All statistical analyses were performed using SAS version 9.4 (SAS Institute, Cary, NC).

Ca^{2+} imaging data were processed using ImageJ and Origin software. Line scanning images of Ca^{2+} were normalized for baseline fluorescence [10,17]. Analysis of I_{Na} was performed using pCLAMP9 software (Molecular Devices, Sunnyvale, CA). ECG recordings were analyzed using the LabChart 7.3 program (ADInstruments), while intracardiac recordings using the DSI ACQ-7700 - acquisition interface (Data Sciences

International). The Wilcoxon-Mann-Whitney or Wilcoxon signed rank test was used to determine *p* values for single comparisons. One-way ANOVA with the Holm test for post hoc testing was used for multiple comparisons (data presented as mean ± standard error of the mean). If the data distribution failed normality tests with the Shapiro-Wilk test statistical analysis of the data was performed using a Friedman rank sum test or Kruskal-Wallis 1-way analysis of variance for paired and unpaired data, respectively. The Conover correction with further adjustment by the Benjamini-Hochberg false discovery rate method was applied to adjust for multiple comparisons. Data presented as median with 25th and 75th percentiles (box) and 10th and 90th percentiles (whiskers). A Fisher's exact test was used to test differences in nominal data. A $p<0.05$ was considered statistically significant.

Supplemental Figures

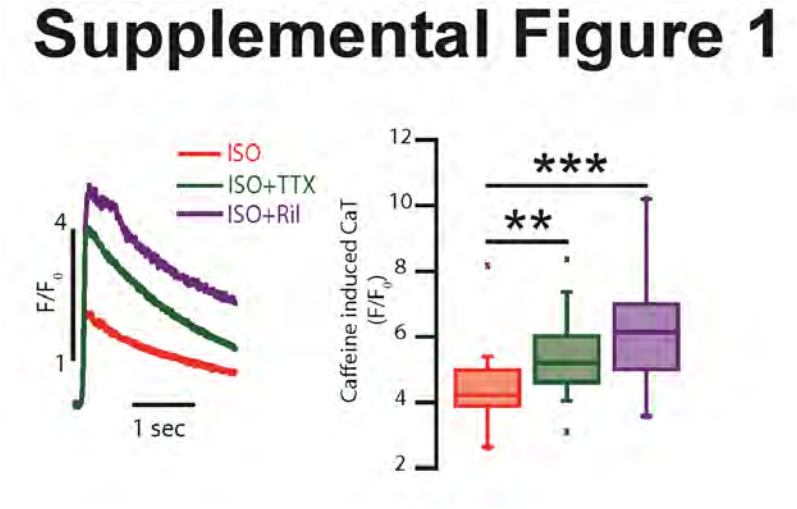

Fig. S1: Inhibition of nNa_v increases SR Ca^{2+} load in R33Q atrial myocytes. Representative caffeine-induced (20 mM) Ca^{2+} transients (CaT; left) recorded in field stimulated R33Q atrial cardiomyocytes. (Right) Summary date reveal that TTX (100 nM; green) and riluzole (Ril; 10 µM; purple) increased CaT relative to isopreteranol (ISO; 100 nM) exposed myocytes (red; n= 20, 21 and 14 cells from N = 10, 8, 6 animals for ISO, ISO-TTX, and ISO-Ril, respectively. p = 0.0011 Kruskal-Wallis test; ** p = 0.0041, *** p = 0.0008).

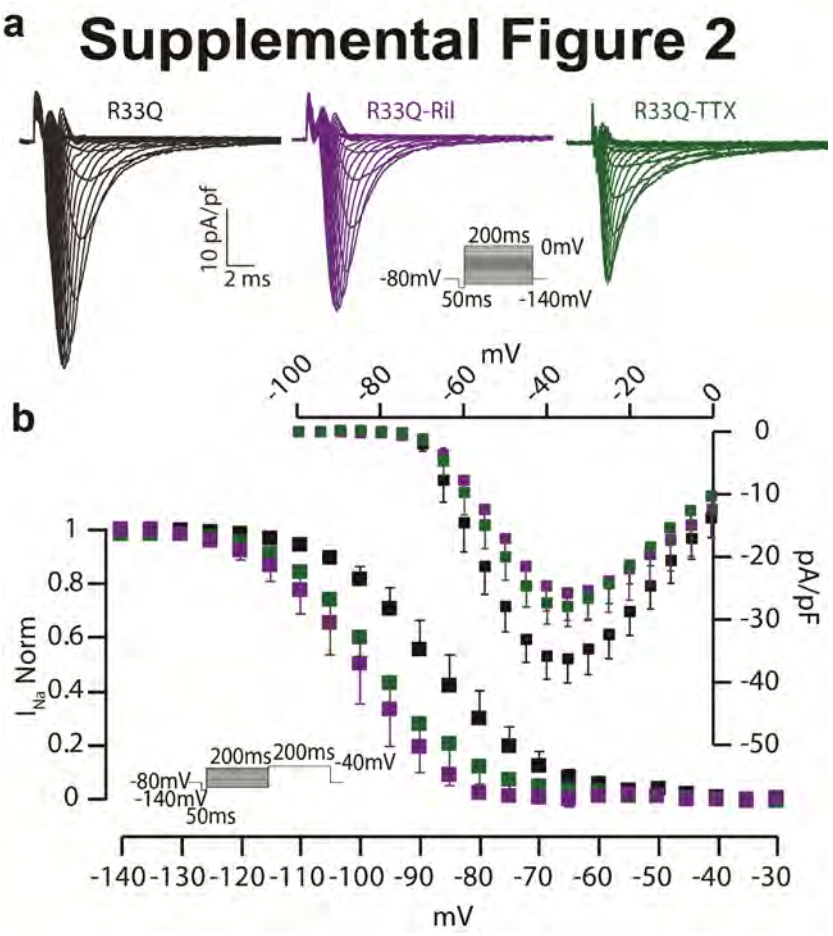

Fig. S2: Effect of nNa_v blockade with TTX and riluzole on Na^+ current in R33Q atrial myocytes. **(a)** Representative inward Na^+ currents (I_{Na}) were elicited by a protocol presented in the inset before (black) or after addition of riluzole (Ril, 10μM; purple) or tetrodotoxin (TTX, 100nM; green). **(b)** (Top) Corresponding voltage dependent activation and inactivation relationship. Addition of Ril or TTX resulted in a reduced maximal I_{Na} density relative to untreated cells (peak I_{Na} at -35mV of -36.4±3.7 pA/pF vs. -25.8±4.4 and -28.1±3.0 pA/pF for control, Ril and TTX, respectively; p = 0.0002 Kruskal-Wallis rank sum test, n = 13, 8 and 8 cells from 8, 4 and 5 mice for R33Q, Ril and TTX, respectively) Normalized voltage dependent inactivation relationships (bottom) demonstrated a hyperpolarizing shift in the $V_{1/2}$ during Ril and

TTX exposure (purple and green squares, respectively; $V_{1/2}$ -87.2±3.7 mV vs. -98.1±3.0 and -95.9±3.2 mV for R33Q, Ril and TTX respectively; p = 0.0345 Kruskal-Wallis rank sum test, n = 7, 5 and 8 cells from 5, 3 and 5 mice for R33Q, Ril and TTX, respectively).

Supplemental Figure 3

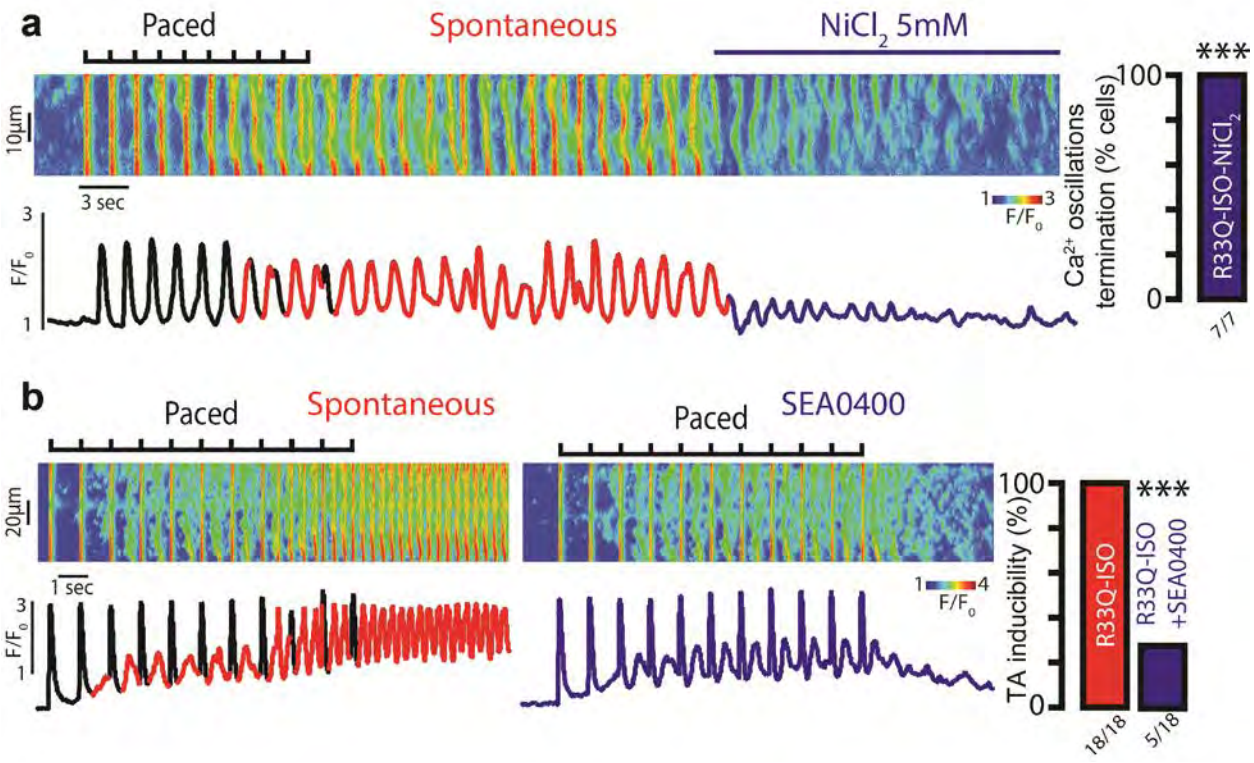

Fig. S3: Inhibition of NCX prevents induction of aberrant, repetitive Ca^{2+} oscillations in R33Q atrial myocytes. (a) Representative examples of the line-scan images and corresponding Ca^{2+} transients (CaT) recorded in field stimulated R33Q atrial cardiomyocytes loaded with Ca^{2+} indicator, Fluo-3 AM. Cells were treated with isopreteranol (Iso, 100 nM) and subsequently $NiCl_2$ (5 mM). NiCl2 abolished Ca^{2+} oscillations (number of cells tested depicted under the corresponding bars; ***p < 0.0081 McNemar's test) **(b)** Treatment of Iso (100 nM)-exposed R33Q atrial myocytes with 1 μM SEA0400 significantly reduced the incidence of aberrant, repetitive Ca^{2+} oscillations (number of cells tested depicted under the corresponding bars, N = 8 animals for Iso and Iso-SEA0400; ***p = 0.0003 McNemar's test).

Supplemental Figure 4

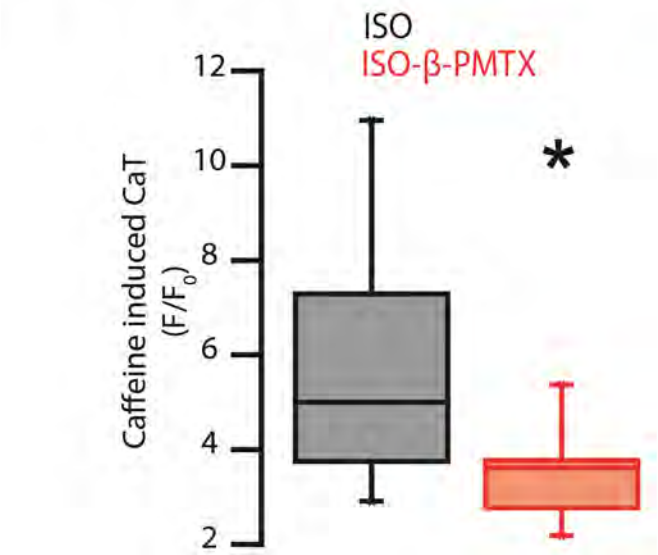

Fig. S4: Augmentation of nNa_v reduces SR Ca^{2+} load in WT atrial myocytes. β-PMTX (40 μM; red) reduced caffeine-induced (20 mM) CaT relative to isopreteranol (ISO; 100 nM; black) exposed WT myocytes (n= 9 cells from N = 4 animals for ISO and ISO-β-PMTX. *p = 0.0400 Wilcoxon ran sum test).

Supplemental Figure 5

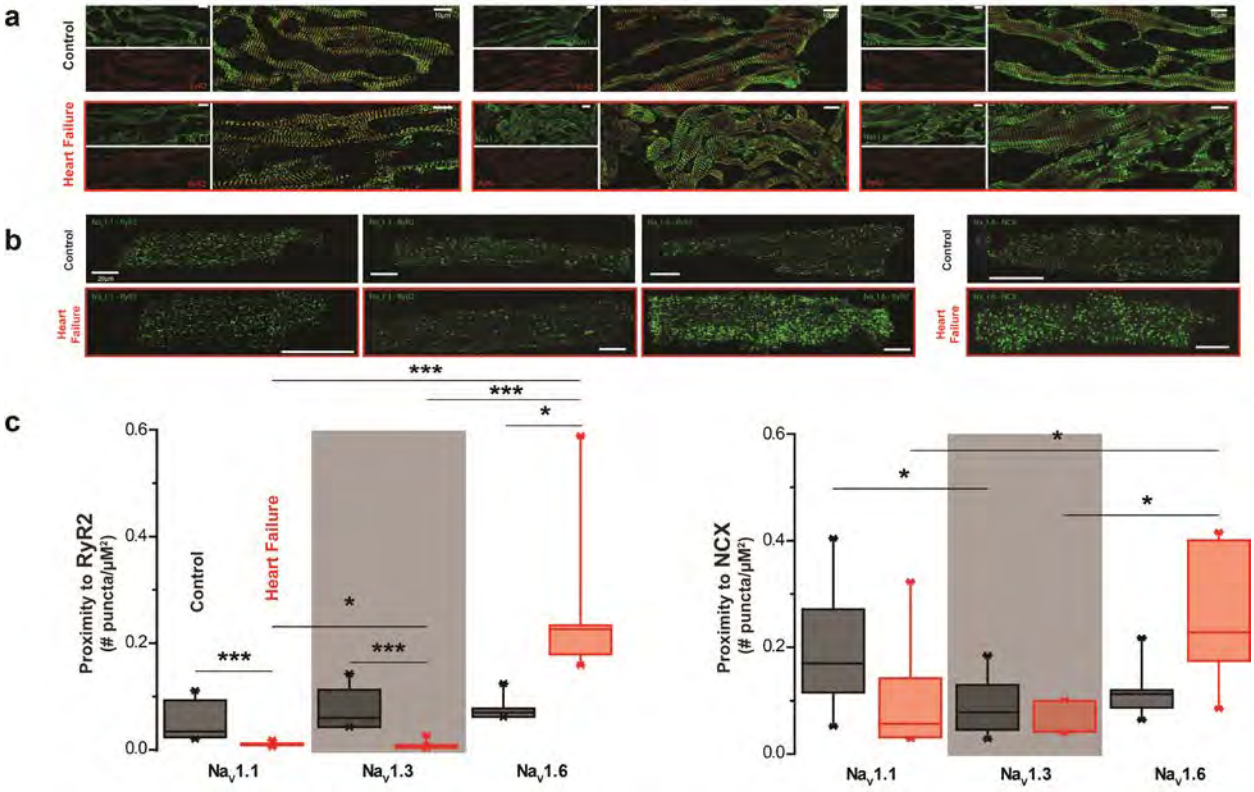

Fig. S5: Increased colocalization of nNa$_V$s and RyR2 in canine heart failure atrial myocytes. Representative confocal images of failing (bottom) and non-failing (top) canine atrial sections co-labeled for RyR2 (red; bottom) and various Na$_V$ isoforms (Na$_V$1.x, green; top). **(b)** Representative confocal images of failing (bottom) and non-failing (top) canine atrial myocytes showing fluorescent proximity ligation assay (PLA) signal for RyR2 (left) and NCX (right) with different nNa$_V$ isoforms (Na$_V$1.x). **(c)** Summary of number of PLA punctae/μm^2 ($p < 0.0001$ Kruskal-Wallis test for Na$_V$1.x-RyR2; ***$p < 0.0001$, *$p = 0.0331$ for Na$_V$1.6-RyR2 control vs. Na$_V$1.6-RyR2 HF, $p = 0.0304$ for Na$_V$1.1-RyR2 HF vs. Na$_V$1.3-RyR2 HF; n = 1223, 963, and 2263 punctae from n = 7, 4, and 7 control dog cells and n = 211, 271, and 3850 punctae from n = 8, 13, and 5 HF dog cells for Nav1.1, 1.3 and 1.6, respectively. $p = 0.0065$ Kruskal-Wallis

test for $Na_V1.x$-NCX; $*p = 0.0183$ for $Na_V1.1$-NCX control vs. $Na_V1.3$-NCX control, $*p = 0.0358$ for $Na_V1.1$-NCX HF vs. $Na_V1.6$-NCX HF, $*p = 0.0134$ for $Na_V1.3$-NCX HF vs. $Na_V1.6$-NCX HF; n = 4893, 2730, and 3960 punctae from n = 10, 10, and 10 control dog cells and n = 1110, 1362, and 2204 cells from n = 5, 6, and 5 HF dog cells for Nav1.1, 1.3 and 1.6, respectively.